ANL-CEN-RSD--82-1

DE83 000930

Distribution Category:
General, Miscellaneous, and
Progress Reports (Nuclear)
(UC-2)

ANL-CEN-RSD-82-1

ARGONNE NATIONAL LABORATORY
9700 South Cass Avenue
Argonne, Illinois 60439

VAPOR PRESSURES AND VAPOR COMPOSITIONS IN EQUILIBRIUM WITH HYPOSTOICHIOMETRIC PLUTONIUM DIOXIDE AT HIGH TEMPERATURES

by

David W. Green, Joanne K. Fink, and Leonard Leibowitz

Chemical Engineering Division

June 1982

TABLE OF CONTENTS

LIST OF FIGURES

LIST OF TABLES

VAPOR PRESSURES AND VAPOR COMPOSITIONS IN EQUILIBRIUM WITH HYPOSTOICHIOMETRIC PLUTONIUM DIOXIDE AT HIGH TEMPERATURES

by

David W. Green, Joanne K. Fink, and Leonard Leibowitz

ABSTRACT

Vapor pressures and vapor compositions in equilibrium with a hypostoichiometric plutonium dioxide condensed phase have been calculated for the temperature range $1500 \leq T \leq 4000$ K. Thermodynamic functions for the condensed phase and for each of the gaseous species were combined with an oxygen-potential model to obtain the partial pressures of O_2, O, Pu, PuO, and PuO_2. New thermodynamic functions for the solid oxide were calculated from available information and from new estimates of the heat capacity of the liquid. Thermodynamic functions for the vapor species were calculated previously. A suitable oxygen-potential model has been used previously for the solid hypostoichiometic plutonium dioxide; we have extended this model into the liquid region using several alternative methods. The effects of these alternatives on the calculated oxygen pressures have been examined in detail. Estimates that resulted in relatively large uncertainties were required. The calculated oxygen pressures were found to increase very rapidly as stoichiometry is approached. At least part of this increase is a consequence of the exclusion of Pu^{6+} from the model of the condensed phase. No reliable method was found to estimate the importance of this ion, whose existence has not been established in the plutonium/oxygen system but whose effects are expected to increase greatly with temperature, similar to those of U^{6+} in the uranium/oxygen system. As a result of large oxygen potentials at high temperatures, extremely high total pressures that produced unreasonably high vapor densities were calculated. The highest temperature for which meaningful results could be calculated was limited to 4000 K, and the range of oxygen-to-metal ratios was 1.70 to 1.994. A major conclusion derived from these calculations is that the vapor in equilibrium with hypostoichiometric plutonium dioxide is poorly approximated as PuO_2 for most of the temperature and composition range of interest. Another conclusion is that the vapor is much more oxygen-rich than the condensed phase with which it is in equilibrium. Both of these conclusions were also made for the uranium/oxygen system, but the plutonium/oxygen system is even more oxygen-rich. The limitations of this approach and some recommendations for additional work are presented. The implications of these calculations for the technologically important $(U,Pu)O_{2-x}$ system are also discussed.

I. INTRODUCTION

One of the most important thermophysical properties of reactor fuel in reactor safety analysis is vapor pressure, for which data are needed for temperatures above 3000 K. We have recently completed an analysis of the vapor pressure and vapor composition in equilibrium with the hypostoichiometric uranium dioxide condensed phase, [1] and we present here a similar analysis for the plutonium/oxygen system.

Over the past twenty years, considerable experimental and theoretical attention has been devoted to the thermodynamics of the uranium oxide, the mixed uranium-plutonium oxide, and the plutonium oxide systems because of their importance to nuclear reactors. Although the plutonium/oxygen system is the least studied of these, many empirical data are now available, and, in some cases, more than one analysis of the same data is available. Nevertheless, considerable uncertainty remains about certain key properties. Potter and Rand, who recently reviewed the status of the thermodynamics of the plutonium/oxygen system, [2] point out that "the Pu_2O_3-PuO_2 phase diagram is still not well defined," that "there has been little fresh work to change our picture of the vaporization behavior of the plutonia phase" since the analysis of Rand [3] in 1966, and that values for partial molar quantities, particularly the oxygen-to-metal ratio near (O/M) = 2.00, are not very well known. In view of these uncertainties in the solid region, it is inevitable that any attempt to extrapolate into the liquid region will involve considerable uncertainty. We have, however, attempted to present a rational and consistent procedure whereby such an extrapolation may be performed. As improved data become available, the extrapolated values obtained by our procedures can be refined to take them into account. We have benefited from the earlier analysis [1] of the uranium/oxygen system in that many of the principles and alternatives of the analysis have been tested.

Defect models of various kinds have been proposed for plutonium dioxide (as well as for the mixed oxide). The characteristics of these models have also been summarized by Rand and Potter.[2] While we can accept their suggestion that the best model is the one with the highest product of ease of application times reliability of results, we come to a different conclusion regarding which model best meets this criterion.

The process we have followed is identical with the one we used previously for the uranium/oxygen system [1] and is summarized by the procedure that is shown in Fig. 1. Thermodynamic functions for the gas-phase molecules were obtained previously [4] from experimental spectroscopic data and estimates of molecular parameters. The functions for the condensed phase have been calculated from an assessment of the available data, including the heat capacity as a function of temperature. The oxygen potential is found from extension into the liquid phase of a model that was devised for the solid phase. Thus, we have all the information needed to apply the procedure outlined in Fig. 1.

The method outlined in Fig. 1 is not the only method of obtaining the required vapor pressures and vapor compositions at very high temperatures; however, it can be applied conveniently to a large portion of the temperature and composition range of interest. Alternative methods depend upon different variables and different measurements. The results obtained by our procedure

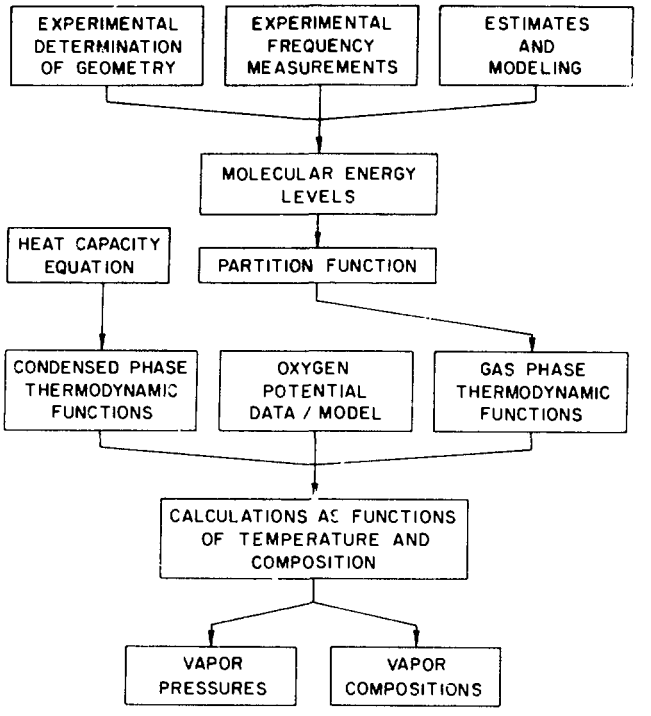

Fig. 1. Procedure for Calculation of Vapor Pressures from Spectroscopic Data

can be usefully compared to experimental data as they become available. Experimental methods for studying vapor pressure at very high temperatures, such as laser-pulse heating techniques, have uncertainties in both the experimental measurements and in the interpretation of the measurements. The method outlined in Fig. 1 also has uncertainties, most of which are different from those associated with empirical techniques. Thus, comparison of our calculated results with measured data should help define the uncertainties in each approach. Ultimate agreement among the results from different methods should reduce the uncertainty in the vapor pressures and vapor compositions at high temperatures.

For the uranium/oxygen system there is quite good agreement between the results obtained by the method outlined in Fig. 1 and many of the experimental data.[1] For the plutonium/oxygen system, fewer experimental data exist; so that, to some degree, the calculated results obtained here should be viewed as an evaluation of the consequence of accepting various models and data.

The procedure we have applied has a sound basis, namely the laws of thermodynamics. The uncertainties in our results are primarily the consequence of incomplete data rather than of uncertainties in the procedures shown in Fig. 1. If all required empirical data were measured, the use of the procedures in Fig. 1 would be simply an application of well-established

thermodynamic relationships. Because empirical data are not available for all the parameters, required values are obtained using estimates and models that could be characterized as "theoretical," "empirical," or "semiempirical." However, we feel the overall procedure is best described as "calculational" or "applied" rather than as "theoretical."

In this report we describe: (1) the gas-phase thermodynamic functions; (2) the condensed-phase thermodynamic functions; (3) the oxygen potential (and the phase boundaries that are consistent with it); and (4) the resulting vapor pressure and composition as functions of temperature and composition of the condensed phase.

II. METHODS

A. General

The methods we have used to calculate the vapor pressures and vapor compositions at high temperatures are the same as those used previously [1] for the U/O system. The total pressure, p(total), in equilibrium with a PuO_{2-x} condensed phase is

$$p(\text{total}) = p(O) + p(O_2) + p(Pu) + p(PuO) + p(PuO_2) \tag{1}$$

where only the neutral species are considered (ions are considered in Section II.F). The oxygen-to-plutonium molar ratio in the gas phase, R(gas), is

$$R(\text{gas}) = \frac{p(O) + 2p(O_2) + p(PuO) + 2p(PuO_2)}{p(Pu) + p(PuO) + p(PuO_2)} \tag{2}$$

The set of partial pressures given by Eq. (1) must satisfy equilibria among themselves and with the condensed phase. Of the several possible choices of independent equilibria, the following set is a convenient one:

$$O_2(g) \rightleftharpoons 2O(g) \tag{3}$$

$$\frac{x}{2} O_2(g) + PuO_{2-x}(c) \rightleftharpoons PuO_2(g) \tag{4}$$

$$PuO_2(g) \rightleftharpoons PuO(g) + 1/2\ O_2(g) \tag{5}$$

$$PuO_2(g) \rightleftharpoons Pu(g) + O_2(g) \tag{6}$$

where c represents the condensed phase and g represents the gas phase.

If we know the oxygen pressure, $p(O_2)$, from the oxygen potential (Section II.C), the required partial pressures may be obtained from Eqs. (3)-(6), in sequence, using the following relationships:

$$\ln p(O) = 1/2 \ln p(O_2) - \Delta G_f^\circ(O)/RT \quad (7)$$

$$\ln p(PuO_2) = \frac{x}{2} \ln p(O_2) + [\Delta G_f^\circ(PuO_{2-x},c) - \Delta G_f^\circ(PuO_2,g)]/RT \quad (8)$$

$$\ln p(PuO) = [\Delta G_f^\circ(PuO_2,g) - \Delta G_f^\circ(PuO,g)]/RT - 1/2 \ln p(O_2) + \ln p(PuO_2) \quad (9)$$

$$\ln p(Pu) = [\Delta G_f^\circ(PuO_2,g) - \Delta G_f^\circ(Pu,g)]/RT - \ln p(O_2) + \ln p(PuO_2) \quad (10)$$

B. Thermodynamic Functions of the Gases

Tabulated data were used in a least-squares fitting procedure to derive an analytical equation for ΔG_f° of each vapor species as a function of temperature. For the plutonium oxide vapor species, the data calculated from spectroscopic data [4] were used; for O(g) and O_2(g), the JANAF data [5] were used; and for Pu(g), data from the compilation of Oetting et al. [6] were used. The coefficients of the equations for ΔG_f° of the gaseous species are included in Table 1. Also included in Table 1 is the equation for $\Delta G_f^\circ(PuO_2,c)$ that was derived from the tabulated data in Table 2 by a least-squares fitting procedure. The methods and data used to obtain Table 2 are described in Section II.E.1.

Table 1. Coefficients of the Equation ΔG_f° (in kJ·mol^{-1}) = $A + BT + CT^2 + DT^3 + E/T + F\cdot\ln(T)$. (℣ represents 298.15 K)

Species	T-range, K	A	B	C	D	E	F
O(g)	℣-1400	252.36	-6.2747×10^{-2}	-1.3294×10^{-6}	—	-527.69	—
	1400-6000	259.03	-6.7710×10^{-2}	-1.6525×10^{-8}	—	-3747.4	—
Pu(g)	1000-3605	260.58	-7.9957×10^{-2}	-2.4343×10^{-6}	—	12715	6.8126
	3605-6000	0.00	—	—	—	—	—
PuO(g)	1000-3605	-106.88	-6.4867×10^{-2}	3.4979×10^{-6}	—	—	—
	3605-6000	-452.62	3.0418×10^{-2}	3.6209×10^{-6}	—	—	—
PuO_2(g)	1000-3605	-481.09	2.1026×10^{-2}	2.3283×10^{-6}	—	—	—
	3605-6000	-783.92	8.9630×10^{-2}	7.6481×10^{-6}	-2.9487×10^{-10}	—	—
PuO_2(c)	913-2701	-1060.9	2.0521×10^{-1}	-6.0130×10^{-6}	—	—	—
	2701-3605	-918.62	1.3644×10^{-1}	—	—	—	—
	3605-6000	-1241.0	2.1943×10^{-1}	2.0882×10^{-6}	-8.9622×10^{-11}	—	—

Table 2. Thermodynamic Functions of the Plutonium Dioxide Condensed Phase (Units for columns 2-5 are $J \cdot K^{-1} \cdot mol^{-1}$ and for columns 6-9 are $kJ \cdot mol^{-1}$.)

T,K	C_p°	S°	$-\left(\frac{G^\circ-H_0^\circ}{T}\right)$	$-\left(\frac{G^\circ-H_{298}^\circ}{T}\right)$	$H^\circ-H_0^\circ$	$H^\circ-H_{298}^\circ$	ΔH_f°	ΔG_f°
0	0.0	0.0	INF	INF	0.0	-10.8	-1052.7	-1052.7
298.15	66.24	66.1	30.0	66.1	10.8	0.0	-1057.7	-999.5
300	66.49	66.5	30.2	66.1	10.9	0.1	-1057.7	-999.2
400	76.43	87.2	41.9	68.9	18.1	7.3	-1060.4	-979.7
500	81.98	104.9	52.8	74.4	26.1	15.3	-1059.6	-959.7
600	85.51	120.2	62.8	80.7	34.4	23.7	-1058.7	-939.8
700	88.01	133.5	71.9	87.4	43.1	32.3	-1057.0	-920.1
800	89.94	145.4	80.4	93.9	52.0	41.2	-1056.9	-900.6
900	91.52	156.1	88.2	100.2	61.1	50.3	-1054.6	-881.2
913	91.70	157.4	89.2	101.0	62.3	51.5	-1057.2	-878.7
913	91.70	157.4	89.2	101.0	62.3	51.5	-1060.0	-878.7
1000	92.88	165.8	95.5	106.3	70.3	59.5	-1055.8	-861.8
1100	94.10	174.7	102.3	112.1	79.7	68.9	-1054.2	-842.4
1200	95.22	183.0	108.7	117.7	89.1	78.3	-1052.5	-823.3
1300	96.26	190.6	114.7	123.0	98.7	87.9	-1050.8	-804.2
1400	97.26	197.8	120.4	128.1	108.4	97.6	-1048.9	-785.3
1500	98.22	204.6	125.8	133.0	118.2	107.4	-1047.0	-766.5
1600	99.15	210.9	130.9	137.6	128.0	117.2	-1045.1	-747.9
1700	100.05	217.0	135.8	142.1	138.0	127.2	-1043.0	-729.4
1800	100.94	222.7	140.5	146.5	148.0	137.3	-1040.9	-711.0
1900	101.82	228.2	144.9	150.6	158.2	147.4	-1038.7	-692.8
2000	102.68	233.4	149.2	154.6	168.4	157.6	-1036.5	-674.6
2100	103.53	238.5	153.4	158.5	178.7	167.9	-1034.2	-656.6
2200	104.38	243.3	157.3	162.2	189.1	178.3	-1031.8	-638.6
2300	105.22	248.0	161.2	165.9	199.6	188.8	-1029.4	-620.8
2400	106.05	252.5	164.9	169.4	210.1	199.4	-1027.0	-603.1
2500	106.88	256.8	168.5	172.8	220.8	210.0	-1024.4	-585.5
2600	107.71	261.0	172.0	176.1	231.5	220.7	-1021.8	-568.0
2700	108.53	265.1	175.3	179.3	242.3	231.6	-1019.2	-550.6
2701	108.54	265.1	175.4	179.4	242.4	231.7	-1019.1	-550.4
2701	96.00	300.0	175.4	179.4	336.8	326.0	-924.8	-550.4
2800	96.00	303.5	179.8	183.7	346.3	335.5	-923.4	-536.7
2900	96.00	306.9	184.2	187.9	355.9	345.1	-922.0	-522.9
3000	96.00	310.1	188.3	191.9	365.5	354.7	-920.6	-509.2
3100	96.00	313.3	192.3	195.8	375.1	364.3	-919.2	-495.5
3200	96.00	316.3	196.1	199.5	384.7	373.9	-917.9	-481.8
3300	96.00	319.3	199.8	203.1	394.3	383.5	-916.6	-468.2
3400	96.00	322.1	203.4	206.5	403.9	393.1	-915.2	-454.7
3500	96.00	324.9	206.8	209.9	413.5	402.7	-913.9	-441.1
3600	96.00	327.6	210.1	213.1	423.1	412.3	-912.7	-427.6
3605	96.00	327.8	210.3	213.3	423.6	412.8	-912.6	-427.0

(contd)

Table 2. (contd)

T,K	C_p°	S°	$-\left(\frac{G^\circ-H_0^\circ}{T}\right)$	$-\left(\frac{G^\circ-H_{298}^\circ}{T}\right)$	$H^\circ-H_0^\circ$	$H^\circ-H_{298}^\circ$	ΔH_f°	ΔG_f°
3605	96.00	327.8	210.3	213.3	423.6	412.8	-1260.8	-427.C
3700	96.00	330.3	213.3	216.2	432.7	421.9	-1261.3	-405.0
3800	96.00	332.8	216.4	219.3	442.3	431.5	-1261.9	-381.9
3900	96.00	335.3	219.4	222.2	451.9	441.1	-1262.5	-358.7
4000	96.00	337.7	222.4	225.1	461.5	450.7	-1263.1	-335.6
4100	96.00	340.1	225.2	227.8	471.1	460.3	-1263.9	-312.4
4200	96.00	342.4	228.0	230.5	480.7	469.9	-1264.6	-289.2
4300	96.00	344.7	230.7	233.2	490.3	479.5	-1265.4	-265.9
4400	96.00	346.9	233.3	235.7	499.9	489.1	-1266.2	-242.7
4500	96.00	349.0	235.8	238.2	509.5	498.7	-1267.0	-219.4
4600	96.00	351.2	238.3	240.7	519.1	508.3	-1267.8	-196.1
4700	96.00	353.2	240.7	243.0	528.7	517.9	-1268.6	-172.8
4800	96.00	355.2	243.1	245.4	538.3	527.5	-1269.4	-149.5
4900	96.00	357.2	245.4	247.6	547.9	537.1	-1270.1	-126.2
5000	96.00	359.2	247.7	249.8	557.5	546.7	-1270.9	-102.8
5100	96.00	361.1	249.9	252.0	567.1	556.3	-1271.5	-79.4
5200	96.00	362.9	252.0	254.1	576.7	565.9	-1272.2	-56.1
5300	96.00	364.8	254.1	256.2	586.3	575.5	-1272.8	-32.7
5400	96.00	366.6	256.2	258.2	595.9	585.1	-1273.4	-9.3
5500	96.00	368.3	258.2	260.2	605.5	594.7	-1273.9	14.2
5600	96.00	370.0	260.2	262.1	615.1	604.3	-1274.3	37.6
5700	96.00	371.7	262.2	264.0	624.7	613.9	-1274.7	61.0
5800	96.00	373.4	264.1	265.9	634.3	623.5	-1275.0	84.5
5900	96.00	375.1	265.9	267.8	643.9	633.1	-1275.3	108.0
6000	96.00	376.7	267.8	269.6	653.5	642.7	-1275.5	131.4

C. Oxygen Potentials

1. Solid Phase

Considerable attention has been devoted to the temperature and composition dependence of the oxygen potential, $\Delta\bar{G}^\circ(O_2)$, for the solids PuO_{2-x} and $(U,Pu)C_{2-x}$.[2] For the calculation of vapor pressures and vapor compositions at high temperature, we sought an oxygen-potential model that has a sound physical basis and is sufficiently uncomplicated to permit reliable extrapolation into the liquid region. The procedure chosen is analogous to that used previously [1] for UO_{2-x}. In this section, we define and evaluate an oxygen-potential model for the PuO_{2-x} solid phase that is consistent with experimental data and has a small number of adjustable parameters. In the following section, we extend this model to the PuO_{2-x} liquid phase and examine various methods of evaluating the adjustable parameters for the liquid model.

Statistical-mechanical models for the temperature and composition dependences of the oxygen potential [7-10] are not well suited to the calculation of oxygen pressures at high temperatures for two reasons. These models generally involve a large number of parameters so that extrapolation to high

temperatures is unreliable even if the model describes the data very well at low temperatures. Furthermore, the physical basis of these models includes effects due to the lattice structure of the condensed phase and, thus, makes them poor candidates for application to the liquid. Quasi-chemical models [11-15] are better suited for our application, although there are problems with this approach as well. [16]

We have chosen the model devised by Blackburn [11] for solid PuO_{2-x} for three reasons: (1) it fits the available experimental data reasonably well; [11] (2) it has a small number of adjustable parameters for which a physical basis can be provided; and (3) it is analogous to the one that has been successfully applied to the UO_{2-x} system. [1] This model for the solid phase assumes the following equilibrium between oxygen gas and the ions in the lattice:

$$4\ Pu^{4+} + 2\ O^{2-} \rightleftharpoons 4\ Pu^{3+} + O_2(g) \tag{11}$$

From this equilibrium the oxygen pressure may be determined:

$$\ln p(O_2) = 4 \ln (Pu^{4+})/(Pu^{3+}) + 2 \ln (O^{2-}) + \ln K_s \tag{12}$$

where the parentheses indicate ionic concentrations (in moles per mole of Pu) and K_s is the equilibrium constant for Eq. (11):

$$K_s = \frac{(Pu^{3+})^4\ p(O_2)}{(Pu^{4+})^4\ (O^{2-})^2} \tag{13}$$

As Blackburn points out, [11] the choice of tetravalent and trivalent Pu ions for this equilibrium is supported by the data of Atlas and Schlehman [7] and Alexander [17] (i.e., $\ln p(O_2) = -4 \ln x + \text{constant}$). In addition, because Pu_2O_3 is a stable compound, there should be no question about the stability of the trivalent ion. Blackburn also included in his model an equilibrium between trivalent and divalent plutonium. Because our interest lies principally in the region for which $x < 0.1$, the divalent ion concentration is expected to be relatively unimportant. Later in this section we shall demonstrate quantitatively that the effects of Pu^{2+} are indeed insignificant in the region of concern and that this species can be ignored without significantly affecting our results.

In addition to Eq. (12), we have the following equations for conservation of plutonium and charge, respectively:

$$(Pu^{4+}) + (Pu^{3+}) = 1 \tag{14}$$

and

$$2\ (Pu^{4+}) + 1.5\ (Pu^{3+}) = (O^{2-}) \tag{15}$$

Substitution of $(O^{2-}) = 2 - x$ into Eqs. (14) and (15) gives $(Pu^{4+}) = 1 - 2x$ and $(Pu^{3+}) = 2x$; thus, Eq. (12) becomes

$$\ln p(O_2) = 4 \ln [(1 - 2x)/2x] + 2 \ln (2 - x) + \ln K_s \qquad (16)$$

To evaluate K_S, Blackburn assumed $\ln K_S = A_S + B_S/T$, where T is the absolute temperature, and A_S and B_S are constants characteristic of $PuO_{2-x}(s)$ that are consistent with the data of Alexander,[17] Atlas and Schlehman,[7] Markin and McIver,[18] Woodley,[19] Javed,[20] Tetenbaum,[21] and Blackburn.[22] This evaluation gave $B_S = -101600$ and $A_S = 20.8$. We have compared the oxygen potentials calculated using Eq. (16), and these parameter values with more recent unpublished data of Tetenbaum [23] and have found good agreement.

The substitution of $(Pu^{3+}) = 2x$ into Eq. (16) creates a mathematical problem in the first term for the special case of $x = 0$ and a physical problem for all small values of x. We shall consider this problem in more detail in Section II.C.2 and also in this section during the discussion of Pu^{6+}. Since a problem exists for $x = 0$, the discussion and numerical calculations will be limited to cases with $x > 0.005$. Some justification for the numerical value of the limit for x will be given below.

We need to demonstrate that it is valid to neglect the Pu^{2+} ion as we have done in Eqs. (11)-(16). The additional equilibrium considered by Blackburn [11] in his model for the Pu/O system is

$$4\ Pu^{3+} + 2\ O^{2-} \rightleftharpoons 4\ Pu^{2+} + O_2(g) \qquad (17)$$

From the equilibrium constant for this reaction, K_2,

$$K_2 = \frac{(Pu^{2+})^4\ p(O_2)}{(Pu^{3+})^4\ (O^{2-})^2} \qquad (18)$$

we solve for the oxygen pressure:

$$\ln p(O_2) = 4 \ln (Pu^{3+})/(Pu^{2+}) + 2 \ln (O^{2-}) + \ln K_2 \qquad (19)$$

From the free energy of formation of Pu_2O_3 and the temperature dependence of the lower phase boundary for $PuO_{1.5-z}$, z_s, Blackburn [11a] found

$$\ln K_2 = 2\ \Delta G_f^\circ(Pu_2O_3)/3RT - 8/3 \ln(1 - 2z_s) + 4 \ln z_s +$$

$$4/3\ z_s - 2 \ln(1.5) + 4 \ln(2) \qquad (20)$$

Because there were no phase data for the metal-rich Pu_2O_3 phase boundary, Blackburn used the lower phase boundary data of Ackermann and Rauh [24] for Ce_2O_3. He chose an equation for $\Delta G_f^\circ(Pu_2O_3)$ based on the data from

the International Atomic Energy Agency (IAEA) [25] and from Battles and Shinn.[26] With these values he found that $\ln K_2 = -188{,}000/T + 45$; [11a] slightly different values are found in Ref. 11c. This expression for $\ln K_2$ includes a temperature dependence for z_s that cannot be extrapolated into the liquid phase. Blackburn's Eq. (12) in Ref. 11a, which should be corrected to give $\ln z_s = 4.65 - 13910/T$, yields a phase boundary at $PuO_{0.89}$ ($z_s = 0.61$) for T = 2700 K and at $PuO_{0.01}$ for T = 3275 K. Clearly, at high temperatures z_s has no physical meaning. Even at temperatures less than 3000 K, there is good reason to question the extrapolation beyond its applicable range.

Trial calculations were done with x = 0.01 and 0.10 to examine the consequences of including the equilibrium given in Eq. (17) and to test the sensitivity of the results to the choice of z_s. Oxygen potentials were calculated for each of the following four cases:

A. Both K_s and K_2 (evaluated as above) are included.

B. Only K_s is considered [i.e., the model defined by Eqs. (11)-(16)].

C. Both K_s and K_2 (recalculated assuming $z_s = 0.001$) are included.

D. Both K_s and K_2 (recalculated assuming $z_s = 0.1$) are included.

The results of these calculations, which are summarized in Table 3, show very small differences in $\log_{10} p(O_2)$ up to about 3000 K. At higher temperatures, case A differs significantly from the other three, as a direct consequence of incorporating a meaningless temperature dependence for z_s in K_2.

Table 3. Oxygen Pressure Calculated from the Oxygen-Potential Model with Four Assumptions about the Equilibrium [Eq. (17)] Involving Divalent Plutonium. (Case A extrapolates the phase boundary equation into the liquid; case B neglects the divalent plutonium; case C assumes $z_s = 0.001$; and case D assumes $z_s = 0.10$.)

	$\text{Log}_{10}\ p(O_2)$, MPa							
	x = 0.01				x = 0.10			
T,K	A	B	C	D	A	B	C	D
2000	-6.66	-6.66	-6.66	-6.66	-11.04	-11.05	-11.05	-11.05
3000	0.72	0.69	0.69	0.69	-3.45	-3.70	-3.70	-3.68
4000	4.49	4.37	4.37	4.37	0.85	-0.02	-0.02	0.01
5000	6.89	6.58	6.58	6.58	3.67	2.18	2.18	2.23

In the oxygen-potential model that was used for the U/O system, [1] two equilibria for the solid were considered. One of these equilibria is analogous to Eq. (11) and the other involved the U^{6+} ion. We are unaware of evidence for the existence of the Pu^{6+} ion in the oxide system. No PuO_3 molecule was identified in matrix-isolation studies [27] although, with similar experimental methods, the UO_3 molecule was easily observed. [28] No evidence for PuO_3 has been reported in mass spectrometric studies. [29] However, the existence of the Pu^{6+} ion has been established by the observation of the hexafluoride. [3]

Although there is no need to postulate the existence of the Pu^{6+} ion for the oxide system in order to explain the experimental oxygen potentials at low temperature, it is expected that the importance of Pu^{6+} will increase substantially with temperature. For the U/O system the hexavalent state is much more important as the temperature increases, and its effect is to decrease the oxygen pressure. In view of the high oxygen pressures given in Table 3 relative to the U/O system, it is desirable to consider carefully any corrections to the model for the Pu/O system that could be expected to reduce the calculated pressure at high temperatures.

Consider the following equilibrium among the ions in the condensed phase:

$$3\ Pu^{4+} \rightleftharpoons Pu^{6+} + 2\ Pu^{3+} \tag{21}$$

that has the equilibrium constant:

$$K_a = \frac{(Pu^{6+})\ (Pu^{3+})^2}{(Pu^{4+})^3} \tag{22}$$

We assume the same form of the temperature dependence for this equilibrium constant that we have assumed for K_s, namely,

$$\ln K_a = A_a + B_a/T \tag{23}$$

so that we may associate A_a with $\Delta S°/R$ for Eq. (21) and B_a with $-\Delta H°/R$ for Eq. (21). To estimate the values of A_a and B_a, we write Eq. (21) as

$$3\ PuF_4(s) \rightleftharpoons PuF_6(s) + 2\ PuF_3(s) \tag{24}$$

From the thermodynamic data for Eq. (24) at 298.15 K, [3] we find $A_a = -0.856$ and $B_a = -52837$. The effect of including the equilibrium of Eq. (21) with these values of the constants in Eq. (23) is to decrease the oxygen pressure at high temperatures. Table 4 gives some numerical results for the oxygen pressure at 2000-5000 K of $PuO_{1.995}$($x = 0.005$), $PuO_{1.99}$($x = 0.01$), and $PuO_{1.90}$($x = 0.10$). The effect of including hexavalent Pu on the calculated $p(O_2)$ is more significant near stoichiometry and is important only at the higher temperatures. These results support our previous restriction of the model to $x > 0.005$. Although the method used to estimate the values of the constants in Eq. (23) is reasonable, a large uncertainty is

Table 4. Oxygen Pressure Calculated from the Oxygen-Potential Model for the Plutonium/Oxygen Solid System, Including and Excluding Hexavalent Plutonium in the Model

	$Log_{10}p(O_2)$					
	x = 0.005		x = 0.01		x = 0.10	
T,K	Pu^{6+}	No Pu^{6+}	Pu^{6+}	No Pu^{6+}	Pu^{6+}	No Pu^{6+}
2000	-5.44	-5.44	-6.66	-6.66	-11.05	-11.05
3000	1.89	1.92	0.68	0.69	-3.70	-3.70
4000	5.40	5.59	4.14	4.37	-0.02	-0.02
5000	5.81	7.80	5.55	6.58	2.18	2.18

associated with these values. We neglect the equilibrium of Eq. (21) because of the absence of empirical data for the existence of Pu^{6+} in the oxide system and, thus, the absence of a reliable method to evaluate quantitatively its importance. However, the consequences of this choice must be numerically tested.

We have, therefore, chosen Eq. (16) with Blackburn's constants of $A_s = 20.8$ and $B_s = -101600$ to represent the oxygen potential for solid PuO_{2-x}.

2. Liquid Phase

Before developing an explicit model for the oxygen potential, $\Delta\bar{G}^\circ(O_2)$ for the liquid PuO_{2-x}, let us consider, in very general terms, the expected behavior of the oxygen potential and the oxygen partial pressure as solid PuO_{2-x} is melted. Figure 2a shows a phase diagram, similar to that for the U/O system [1] and to that recommended for the Pu/O system, [3] for the melting region. Figure 2b shows the expected temperature dependence of the oxygen pressure in a plot of $\ln p(O_2)$ versus $1/T$. This plot should be nearly linear (in the absence of phase changes) because of the relationship between the oxygen potential and pressure:

$$\Delta\bar{G}^\circ(O_2) = \Delta\bar{H}^\circ(O_2) - T\,\Delta\bar{S}^\circ(O_2) = RT \ln p(O_2)$$

where $\Delta\bar{H}^\circ(O_2)$ and $\Delta\bar{S}^\circ(O_2)$ should be approximately constant for small temperature ranges.

To examine the effects of melting a solid of a given composition, consider the heating of the solid that is represented by the broken vertical line at the composition PuO_{2-a} ($x = a$) in Fig. 2a. The curve marked solid in Fig. 2b represents the change in $\ln p(O_2)$ as a function of $1/T$ corresponding to the equilibrium with the solid. At point X in Fig. 2a, the solid PuO_{2-a}

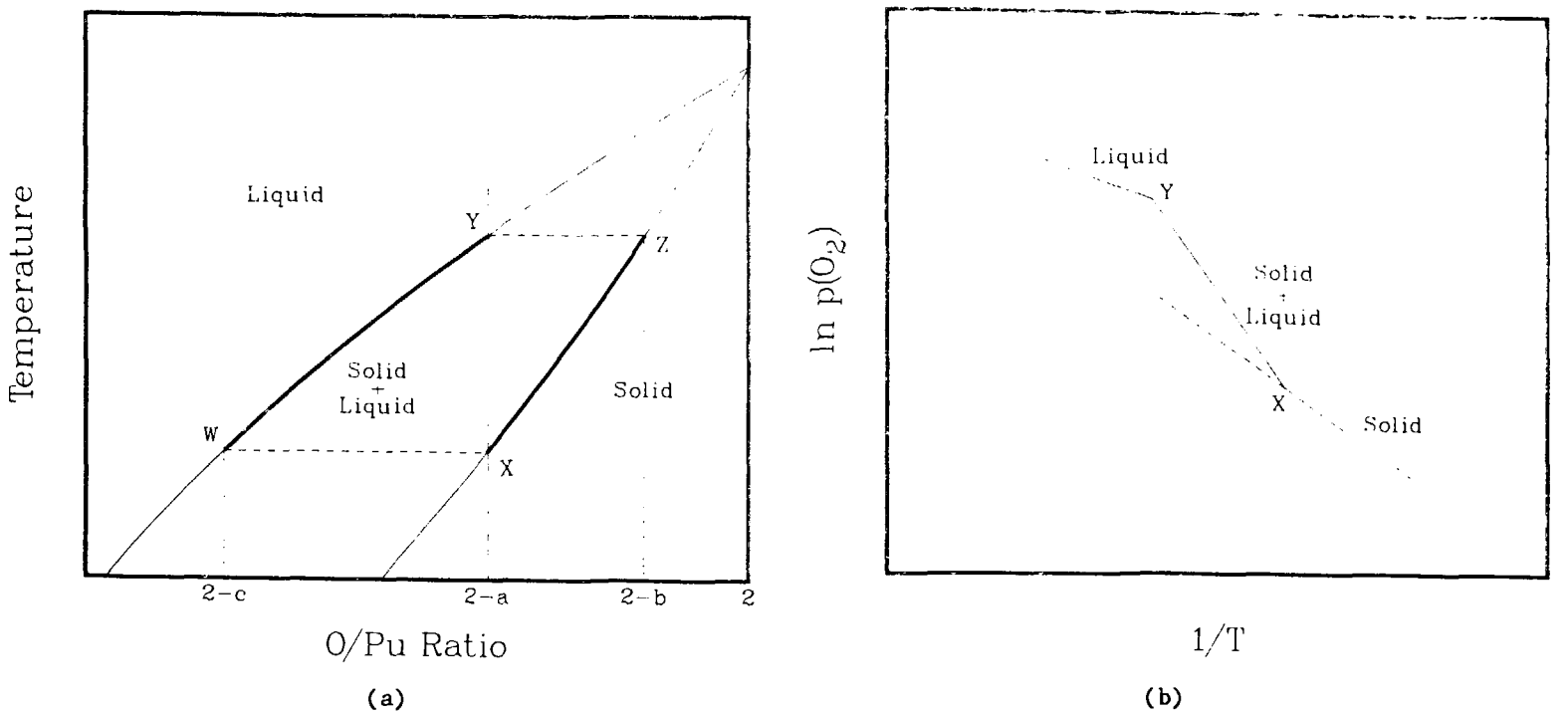

Fig. 2. (a) Schematic Representation of a Portion of the Pu/O Phase Diagram; (b) ln $p(O_2)$ vs. 1/T Corresponding to the Phase Diagram Above. The curve XY in (b) is a portion of a "universal curve" that represents the variation of ln $p(O_2)$ with 1/T for all compositions. Referring to (a), we may heat a solid of composition PuO_{2-d}, where $b < d < a$, until the solidus is reached. At this temperature the oxygen pressure in equilibrium with solid PuO_{2-d} is identical with that in equilibrium with the solid whose original composition was PuO_{2-a} heated to the same temperature. This equality is evident from (a) and the discussion in the text, i.e., the solid PuO_{2-a} exists at this temperature as a two-phase system with overall composition PuO_{2-a} including a solid of composition PuO_{2-d}. Thus, the variation of ln $p(O_2)$ with 1/T for a solid with initial composition PuO_{2-d} would appear in (b) as a curve above the solid portion until the solidus temperature is reached. At this point it has intersected the curve XY and the variation of ln $p(O_2)$ with 1/T is identical with XY and its extension. This analysis holds for all compositions. Thus, we refer to XY as the "universal curve" because, irrespective of initial composition, the variation of ln $p(O_2)$ with 1/T within the two-phase region is given by XY or its extension. The existence of this universal curve is a direct consequence of the dependence of $p(O_2)$ only on the temperature at any point in the two-phase region and not on the initial composition of the heated solid.

begins to melt and three phases (the solid, a liquid of composition PuO_{2-c}, and the vapor) are in equilibrium. Between points X and Y, two condensed phases of different compositions are in equilibrium at every temperature. The solid phase changes composition from PuO_{2-a} to PuO_{2-b} as the system changes from all solid to all liquid. The oxygen potential and ln $p(O_2)$ increase more rapidly with temperature, shown by the curve XY in Fig. 2b, because of the combined effects of increasing temperature and increasing oxygen concentration in the equilibrium solid. The liquid whose composition changes from PuO_{2-c} to PuO_{2-a} between points X and Y must have the same oxygen potential as the solid with which it is in equilibrium. At point Y in Fig. 2a the liquid PuO_{2-a} must have the same oxygen potential as the solid PuO_{2-b}.

When the temperature corresponding to point Y is exceeded, a single-phase (liquid) region of the phase diagram is entered, and the oxygen potential again increases with temperature with no change in composition, corresponding to the liquid curve in Fig. 2b. The liquid curve is nearly linear for the same reason that the solid curve is. However, the slope of the liquid curve is smaller than that of the solid curve because the partial molal enthalpy of oxygen, $\bar{\Delta H}^{\circ}(O_2)$, for the liquid is less than that for the solid. The oxygen potential for the liquid, however, increases relative to the extrapolated solid at point Y by an amount that depends upon the temperature difference between points X and Y and on the functional dependence of the oxygen potential on both the temperature and the composition.

The value for the oxygen potential of the liquid at point Y (and all along the liquidus) is independent of any assumptions about the oxygen-potential model for the liquid. However, if the solidus and liquidus are known, then the functional dependence on temperature and composition of the oxygen potential for the liquid (at least along the liquidus) is fixed by the corresponding functional dependence of the oxygen potential for the solid. It is expected, therefore, that the extrapolated oxygen potential for the metastable solid is lower than that for the stable liquid just above the liquidus temperature. This higher oxygen pressure for the equilibrium with the liquid is contrary to what would be expected for the special case of $x = 0$, for which the metastable phase always has a higher oxygen pressure. With these general expectations in mind, we may now develop an oxygen-potential model for the liquid PuO_{2-x} system.

To extend the oxygen-potential model from the solid phase to the liquid phase, we assume that the model for the solid defined by Eqs. (11)-(16) applies to the liquid with new values of the model parameters. Therefore, we must find a new equilibrium constant K_ℓ that is analogous to K_s. We have considered several methods of evaluating the model parameters (the equation that gives K_ℓ as a function of temperature) from the available data.

In the two-phase (solid + liquid) region, the oxygen potentials of both phases must be equal at every temperature. If we know the variation of composition with temperature for the solidus and liquidus, we can readily calculate K_ℓ as a function of temperature from K_s. Note that this method of determining the temperature-dependence of K_ℓ does not, in general, lead to the same functional form, namely $A + B/T$, as that assumed for K_s. If we equate Eq. (16) and its liquid analog for points along the boundaries of the two-phase region, we find

$$4 \ln (1 - 2x_s)/2x_s + 2 \ln (2 - x_s) + \ln K_s$$

$$= 4 \ln (1 - 2x_\ell)/2x_\ell + 2 \ln (2 - x_\ell) + \ln K_\ell \quad (25)$$

or

$$4 \ln (1 - 2x_s)x_\ell/(1 - 2x_\ell)x_s + 2 \ln (2 - x_s)/(2 - x_\ell) = \ln K_\ell - \ln K_s \quad (26)$$

where x_s and x_ℓ represent the solidus and liquidus compositions of PuO_{2-x_s} and PuO_{2-x_ℓ}, respectively. If reliable equations for x_s and x_ℓ were available, we could calculate K_ℓ using the equation for K_s from Blackburn's analysis of the data for the solid phase.

We can better understand what to expect for K_ℓ by the following analysis. Write Eq. (11) in the form

$$4\ PuO_2(s) \rightleftharpoons 2\ Pu_2O_3(s) + O_2(g) \quad (27)$$

The equilibrium constant for this reaction is given by

$$-RT \ln K = \Delta G^\circ = \Delta H^\circ - T\ \Delta S^\circ \quad (28)$$

An analogous equation may be written so that an equation like Eq. (28) is valid for the liquid as well. The difference between ΔG° for Eq. (28) and ΔG° for its liquid analog becomes

$$\Delta(\Delta G^\circ) = 2\Delta H_m^\circ(Pu_2O_3) - 4\ \Delta H_m^\circ(PuO_2) - T\ [2\ \Delta S_m^\circ(Pu_2O_3) - 4\ \Delta S_m^\circ(PuO_2)] \quad (29)$$

where ΔH_m° and ΔS_m° are the enthalpy and entropy of fusion, respectively, of the indicated compound.

If $\ln K = A + B/T$ for the liquid as well as for the solid, then

$$(A_\ell - A_s) + (B_\ell - B_s)/T = -\Delta(\Delta G^\circ)/RT \quad (30)$$

If the enthalpy and entropy of fusion are independent of temperature, Eqs. (29) and (30) yield

$$\Delta A = A_\ell - A_s = [2\ \Delta S_m^\circ(Pu_2O_3) - 4\ \Delta S_m^\circ(PuO_2)]/R \quad (31)$$

and

$$\Delta B = B_\ell - B_s = -[2\ \Delta H_m^\circ(Pu_2O_3) - 4\ \Delta H_m^\circ(PuO_2)]/R \quad (32)$$

The enthalpies and entropies of fusion that are required for evaluations of Eqs. (31) and (32) may be estimated for PuO_2 and Pu_2O_3 in a manner analogous to that for UO_2. [1] A reasonable estimate for the entropy of fusion was

found [1] to be 1.4nR (n is the number of atoms per molecule, and R is the gas constant), so that we obtain $\Delta A = -2.8$. As discussed below, the value of ΔB depends on the plutonia melting points.

We now examine alternative methods of calculating values of A_ℓ and B_ℓ which were used to calculate oxygen potentials for the liquid with the relationships we have outlined above.

Method A. With both K_S and K_ℓ taken to be of the form A + B/T, Eq. (26) has two unknowns, A_ℓ and B_ℓ (A_S and B_S are known). If two temperatures are selected from the phase diagram in [30] (i.e., two values of x_S and x_ℓ at which the $p(O_2)$ values must be the same), we can solve for A_ℓ and B_ℓ. This procedure, although conceptually satisfactory, fails (1) because there are uncertainties in the phase diagram in the melting region and (2) because the assumed temperature dependences for x_S, x_ℓ, and ln K imply a functional form for ln K_ℓ that is not quite consistent with the A + B/T form that has been assumed. Thus, small variations in the values chosen for x_S and x_ℓ result in different values for the "constant" A_ℓ. Moreover, small changes in the phase boundaries produce physically unreasonable results. We rejected this method of evaluating the parameters for the liquid model because it is too sensitive to yield reliable results with the present state of knowledge about the Pu/O phase diagram.

Method B. We have already calculated a physically reasonable value (-2.8) for ΔA from Eq. (31) by relating it to entropy changes that can be estimated by analogy to other systems. If 2701 K [31] and 2353 K [30] are taken for the melting temperatures $T_m(PuO_2)$ and $T_m(Pu_2O_3)$, respectively, we find $\Delta B = 12434$ from Eq. (32). We have also calculated ΔB and ΔA from Eqs. (31) and (32), assuming that the entropy of fusion was nR (instead of 1.4nR); we obtain $\Delta A = -2.0$ and $\Delta B = 8882$. Oxygen-potential calculations were performed for both of these cases.

The next set of procedures (alternatives C, D, and E below) makes various assumptions about the behavior of PuO_2/Pu_2O_3 solutions. Let us first consider the general equations. The region of interest (small x near 2701 K) can be considered as a dilute solution of Pu_2O_3 in PuO_2. If the solvent (PuO_2) is considered ideal, we can write for the melting region

$$\ln (y_\ell/y_s) = \Delta H_m^\circ(PuO_2)/R \cdot \left[\frac{1}{T_m(PuO_2)} - \frac{1}{T}\right] \qquad (33)$$

where y_ℓ and y_S are the mole fractions of PuO_2 in the liquid and solid. A more severe (probably unrealistic) assumption is that the solute (Pu_2O_3) is ideal as well, whence

$$\ln (1 - y_\ell)/(1 - y_s) = \Delta H_m^\circ(Pu_2O_3)/R \cdot \left[\frac{1}{T_m(Pu_2O_3)} - \frac{1}{T}\right] \qquad (34)$$

Method C. We estimate the value of ΔA from entropy of fusion arguments (using $\Delta S^\circ = 1.4$ nR) and calculate ΔB (which now varies with T) by means of Eqs. (25), (31), and (32). We then extrapolate to the dilute-solution limit ($x_\ell = x_S = 0$) and use the resulting value for ΔB to find B_ℓ.

Method D. We proceed as in method C, but instead of extrapolating to x = 0, we note that the resulting function ($\ln K_\ell - \ln K_S$) is very well represented by an equation of the form $a + b/T + c \ln T$. Because we already have an equation for $\ln K_S$ as a function of T, it is possible to calculate $\ln K_\ell = a_\ell + b_\ell/T + c_\ell \ln T$. To apply the solution model, we require values for the enthalpies of fusion of PuO_2 and Pu_2O_3; these are obtained from Eqs. (31) and (32) by using either of the estimates of entropy of fusion that are given above together with the melting points.

Method E. We accept the solidus from the IAEA [30] phase diagram and calculate the liquidus using only Eq. (33) (assuming an entropy of fusion of 1.4 nR). We then calculate ΔB from Eq. (25) and extrapolate to the dilute-solution limit at x = 0.

Method F. We extrapolate the solid model and parameter values into the liquid region of the phase diagram. Although we do not expect this procedure to be as good as other procedures, it does provide a basis for comparing results.

A summary of the results of these calculations for methods B through F is shown in Table 5, where calculated oxygen pressures are given at several temperatures. Method A was not included in this comparison. This method was rejected earlier because trial calculations showed the derived parameter values and, thus, the values of $\ln p(O_2)$ were too sensitive to the details of the phase diagram. Thus, numerical results depend on what points of the phase diagram were chosen.

3. Summary

Several alternatives for calculating the oxygen potentials of the solid and liquid Pu/O systems have been considered. The conclusions that have been reached in these considerations are summarized here.

1. Blackburn's model [11] for the solid Pu/O system is consistent with empirical data, and it has a physical basis that is similar to the model that was used successfully for the U/O system. [1] We shall use it with the parameter values A = 20.8 and B = -101600. This model is limited to hyposto-ichiometric plutonium dioxide because the concentration of the trivalent ion becomes zero at x = 0.

2. The effects of divalent plutonium ion were included in the solid system, [11] but they are so small in our region of interest relative to the uncertainties that we may safely neglect Pu^{2+} in the following calculations.

3. The hexavalent ion was not previously included in the solid Pu/O system, but is relatively important in the U/O system at high temperatures. [1] Inclusion of Pu^{6+} has the effect of lowering the oxygen pressure, and, for this reason, it would be desirable to include it in the model. However, we choose to exclude Pu^{6+} because it has not been empirically shown to exist in the oxide system. Thus, no reliable method exists to evaluate quantitatively its importance.

Table 5. Oxygen Potential Calculated Using Alternative Methods of Evaluating the Oxygen-Potential Model Parameters for the Liquid Plutonium/Oxygen System

	$Log_{10}p(O_2)$, MPa		
T,K	x = 0.01	x = 0.10	Metnod of Calculation
3000	1.11	-3.28	Method B. $\Delta S = nR$;
4000	4.47	0.07	estimate both enthalpy and
5000	6.48	2.09	entropy of fusion
3000	1.28	-3.11	Method B. $\Delta S = 1.4nR$;
4000	4.50	0.11	estimate both enthalpy and
5000	6.44	2.05	entropy of fusion
3000	1.58	-2.81	Method C. $\Delta S = 1.4nR$;
4000	4.73	0.34	ideal solution limit
5000	6.62	2.23	
3000	2.28	-2.11	Method D. $\Delta S = 1.4$ nR;
4000	4.60	0.21	ideal solvent and solute
5000	4.58	0.19	
3000	2.04	-2.07	Method E. $\Delta S = 1.4$ nR;
4000	5.28	0.89	IAEA solidus with ideal
5000	7.06	2.63	solution limit
3000	0.69	-3.70	Method F. Extrapolation of
4000	4.37	-0.02	solid model to liquid
5000	6.58	2.18	

4. For fusion processes, the effect on the calculated oxygen pressures of the difference between $\Delta S^\circ = nR$ and $\Delta S^\circ = 1.4nR$ is small. We choose to use $\Delta S^\circ = 1.4nR$ as we did for the U/O system. [1]

5. The choice among models for the oxygen potential of the liquid Pu/O system is limited. We extended the model for the solid Pu/O system to the liquid and evaluated new parameter values. This choice is consistent with that made for the U/O system. [1]

6. Several alternative methods for evaluation of the liquid model parameters were considered. Some of the alternatives yielded small differences in $p(O_2)$ for $T < 5000$ K, and in other cases reasons could be determined for not expecting the parameters to be valid at high temperature. No clear preference for one method of evaluating parameters has emerged, in large part because of the absence of high-temperature experimental data needed to test the alternatives. We choose method B of evaluating the liquid model parameters, namely, to estimate both ΔS° and ΔH° of fusion using 1.4nR and to use the relationship between these values and the changes in model parameters, ΔA and ΔB. Thus, $A_\ell = 18.0$ and $B_\ell = -89166$.

7. The very large values of ln $p(O_2)$ that appear in Tables 3-5 suggest that the oxygen-potential model may be limited to lower temperatures for the Pu/O system than for the U/O system. The upper temperature limit cannot be defined precisely, but there is a very high uncertainty for $T > 4000$ K.

D. The Phase Boundaries

The phase boundaries were considered in the previous section as part of the evaluation of the parameters for the liquid oxygen-potential model. At this point, our interest in the phase diagram is solely to define the method by which the calculation of the partial pressures should be done (i.e., the calculations proceed differently depending on whether there is a solid, a liquid, or two phases in equilibrium with the vapor). Because (1) small changes in the phase boundaries have only small effects on the total pressure and vapor composition and (2) the range of T and x values for which the method of calculation will be affected is small, there is little need to have an accurate phase diagram. It is more important to use a phase diagram that is consistent with our method and choice of parameter values.

The solidus, the liquidus, and the oxygen-potential model for the solid and liquid Pu/O system each depend upon the temperature, T, and the composition (x defined by PuO_{2-x}). At each fixed temperature, the oxygen pressure in equilibrium with the solid of composition given by the solidus, x_s, and with the liquid of composition given by the liquidus, x_ℓ, must be the same. Thus, it follows that the T and x dependences of x_s and x_ℓ, as well as the two parts of the oxygen-potential model, are not independent. Because the oxygen-potential model has a greater effect on the vapor pressure and composition at high temperature than do the solidus and liquidus, we have fixed the functional forms and the parameter values for the oxygen-potential model. We choose the IAEA solidus [30] and determine the liquidus that is consistent with it and with the two parts of the oxygen-potential model. In Fig. 3 we compare the solidus and three alternatives for the liquidus. Our choice for the liquidus, which is based on alternative B, for the evaluation of the liquid model parameters is very close to the IAEA liquidus. [30]

The phase diagram that we shall use to define the method of calculation is given in Fig. 4. The following regions are defined by these choices:

Region I: One-phase solid; $T < 2416$ K; $0.005 < x < 0.30$

Region II: One-phase solid; $2416 < T < 2701$; $0.005 < x < x_s$

Region III: Solid and liquid phases; $2416 < T < 2701$; $x_s < x < x_\ell$

Region IV: One liquid phase; $T < 2701$; $x_\ell < x < 0.30$

Region V: One liquid phase; $2701 < T < 5000$; $0.005 < x < 0.30$

The solidus, which is the one recommended by the IAEA, can be represented by the following equation for $2416 < T < 2701$ K:

$$x_s = 9.577 - 6.333 \times 10^{-3}\, T + 1.032 \times 10^{-6}\, T^2 \qquad (35)$$

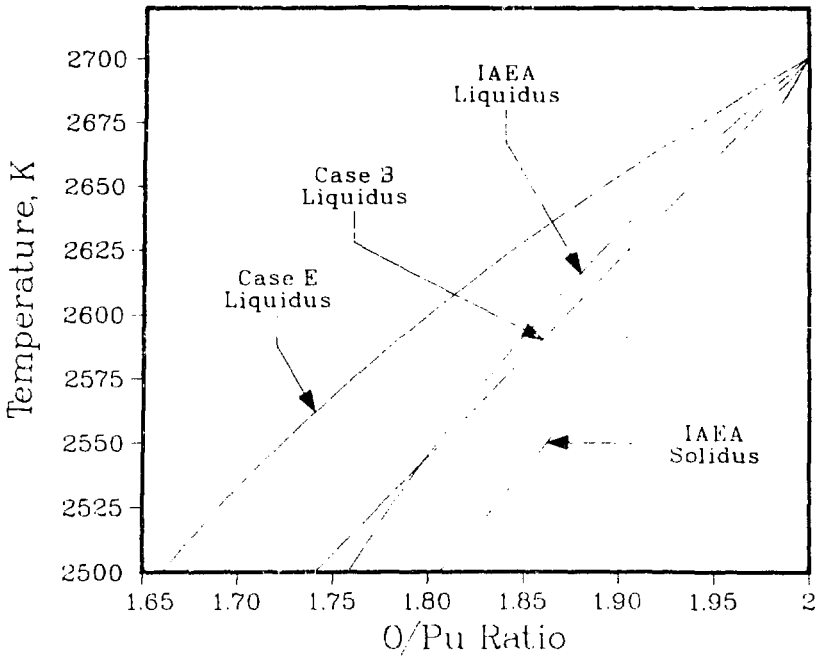

Fig. 3. The IAEA Solidus for the Pu/O Phase Diagram Compared with Alternative Liquidus Curves

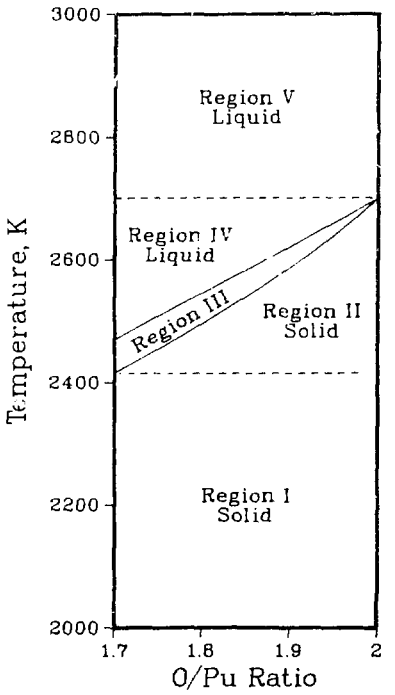

Fig. 4.

Phase Diagram of the Pu/O System

The uncertainty in the value of x_ℓ calculated from Eq. (35), which is probably somewhat less than 0.005, is the result of our inability to read the values of x and T accurately from the graph in Ref. 30. This uncertainty is expected to be very much less than that in the solidus itself. The uncertainty in the solidus equation, Eq. (35), from either source is not a major cause of uncertainty in our results.

The liquidus, which is consistent with Eq. (35) and the two parts of the oxygen-potential model, can be represented by the following equation for $2416 < T < 2701$ K:

$$x_\ell = 5.108 - 2.534 \times 10^{-3}\ T + 2.378 \times 10^{-7}\ T^2 \qquad (36)$$

E. Thermodynamic Functions of the Condensed Phases

1. Plutonium Dioxide

Values of the thermodynamic functions for the condensed phases of plutonium dioxide are given for temperatures up to 6000 K in Table 2. These values were calculated using standard thermodynamic relationships, which have been described previously [1] for the case of UO_2, and using the data that are described here.

The phase-transition temperatures for Pu and PuO_2, which were used to calculate the functions in Table 2, are given in Table 6. To calculate the last two columns in Table 2, data were taken from JANAF [5] for gaseous oxygen and from Oetting et al.[6] for the reference state of the metal.

The heat capacity function for the solid phase is from Fink, [32] namely:

$$C_p^\circ(PuO_2,s) = \frac{87.394\ \theta^2\ \exp(\theta/T)}{T^2 \cdot \{\exp(\theta/T) - 1\}^2} + 0.007956\ T \qquad (37)$$

for C_p° in $J \cdot K^{-1} \cdot mol^{-1}$, $298.15 < T < 2701$ K, and $\theta = 587.41$ K.

This equation assumes there is one solid phase for PuO_2. As shown in Table 7, there is evidence for solid-solid transitions in ThO_2 and in UO_2. In addition, the mixed oxide, $(U,Pu)O_2$, shows a similar transition at about 2750 K. [32] Although the mathematical fit to the experimental enthalpy data for PuO_2 does not indicate a solid-solid phase transition, scatter in the available data [41] in the temperature region where a phase transition may be expected (2160 to 2370 K) makes it impossible to exclude the existence of a phase transition. Additional high-temperature measurements could indicate the presence of a solid-solid phase transition; in that case, the heat capacity of PuO_2 between the phase transition and 2701 K would be significantly higher if PuO_2 is analogous to ThO_2.[40]

The heat capacity for liquid PuO_2 has been estimated using the following thermodynamic relationship:

Table 6. Important Transition Temperatures for the Plutonium Dioxide Condensed Phase

T,K	Phase Transition	Source
395	Pu(α)--Pu(β)	Oetting et al. [6]
480	Pu(β)--Pu(γ)	Oetting et al. [6]
588	Pu(γ)--Pu(δ)	Oetting et al. [6]
730	Pu(δ)--Pu(δ)	Oetting et al. [6]
752	Pu(δ)--Pu(ε)	Oetting et al. [6]
913	Pu(ε)--Pu(ℓ)	Oetting et al. [6]
2701	PuO_2(s)--PuO_2(ℓ)	Aitkin and Evans [31]
3605	Pu(ℓ)--Pu(g)	Calculated from data in [6]

Table 7. Data on Oxide Used to Calculate Thermodynamic Functions of the Condensed Phases

Quantity	ThO_2	UO_2	PuO_2
$\Delta H_f^\circ(298.15)$, kJ·mol^{-1}	-1226.7[a]	-1084.9[b,c]	-1057.7[d]
$S^\circ(298.15)$, J·K^{-1}·mol^{-1}	65.23[a]	77.027[b]	66.13[e]
$H^\circ(298.15) - H^\circ(0)$, kJ·mol^{-1}	10.56[f]	11.28[b]	10.784[e]
T_m, K	3643[a]	3120[g]	2701[h]
ΔH_m°, kJ·mol^{-1}	127.214[i]	74.814[g]	94.319[j]
T(α-β), K	2950[k]	2670[g]	none
$\Delta H^\circ(\alpha-\beta)$, kJ·mol^{-1}	13.807[j]	0.3[g]	none

[a]Ref. [33].
[b]Ref. [34].
[c]Ref. [35].
[d]Ref. [3].
[e]Ref. [36].
[f]Ref. [37].
[g]Ref. [38].
[h]Ref. [31].
[i]Estimated as 1.4 nRT_m
[j]Ref. [39].
[k]Ref. [40].

$$C_p^\circ = C_v^\circ \left[1 + \frac{\alpha_p^2 \cdot V}{C_v^\circ \cdot \beta_T} \right] T \qquad (38)$$

where C_p° is the heat capacity at constant pressure, C_v° is the heat capacity at constant volume, β_T is the isothermal compressibility, V is the molar volume, and α_p is the thermal expansion coefficient. Because none of these thermodynamic parameters has been measured for liquid PuO_2, corresponding values for UO_2 at its melting point have been used with Eq. (38) to estimate the heat capacity of liquid PuO_2.

The values of 10.3×10^{-5} K^{-1} for the thermal expansion coefficient and 3.048×10^{-5} $m^3 \cdot mol^{-1}$ for the molar volume were calculated for liquid UO_2 at its melting point (3120 K) from Drotning's empirical equation for the density of liquid UO_2, [42] which gives the value of 8.859×10^3 $kg \cdot m^{-3}$ at the melting point. The value of 41.19×10^{-12} Pa^{-1} for the isothermal compressibility of UO_2 at its melting point was calculated by Fink et al. [38] from the available data.

The lattice harmonic oscillator contribution of $9R = 75$ $J \cdot mol^{-1} \cdot K^{-1}$ was used in Eq. (38) for C_v°. In contrast to the calculations for UO_2, no electronic contribution to the constant volume heat capacity has been included in this estimate. This difference between PuO_2 and UO_2 is based on the measured difference in enthalpies as functions of temperature. The rapid increase of the enthalpy of UO_2, which occurs above 1500 K and is particularly important within 300 or 400 K of the melting point, has been interpreted as evidence for an electronic contribution. [43] No corresponding evidence exists for an electronic contribution in the data for PuO_2. [32] The difference in enthalpy data between UO_2 and PuO_2 is consistent with the electronic energy-level structures. [44] Other interpretations of the difference in the measured heat capacities between UO_2 and PuO_2 imply that the value of C_v° in Eq. (38) should be smaller for PuO_2 than for UO_2. Thus, our choice of $9R$ for C_v° could be viewed as being a direct consequence of a difference in experimental enthalpy data for UO_2 and PuO_2 and, therefore, as independent of the reason for the difference. However, some understanding of the reason for this difference does help in evaluating the uncertainties in C_p° at high temperature.

If the neglected electronic terms are important, then the true C_v° for PuO_2 liquid will be larger, which would affect all calculated thermodynamic functions for the liquid. Thus, although the C_v° value we have used is consistent with the available experimental data and with our expectations based on the electronic structure, there is an uncertainty associated with this estimate that results in an uncertainty in the calculated vapor pressures at higher temperatures.

Before we substitute the above-mentioned values into Eq. (38), we shall consider one alternative approach. A value of 1.016 is calculated for the Grüneisen constant,

$$\Gamma = \frac{\alpha_p \cdot V}{C_v^\circ \cdot \beta_T} \tag{39}$$

with the values for liquid UO_2 at the melting point. If the commonly used estimate of $\Gamma = 2.0$ [45] were substituted for 1.016, the estimated heat capacity of PuO_2 at constant pressure would be larger by 18%. Because it appears that the thermodynamic properties of PuO_2 resemble UO_2 more closely than other materials, we believe it is more reliable to use the values for V, β_T, and α_p obtained for UO_2 in Eq. (38).

Thus,

$$C_p^\circ(PuO_2,\ell) = 96\ J \cdot mol^{-1} \cdot K^{-1} \tag{40}$$

for all $T > 2701$ K.

Numerical values of thermodynamic parameters that were used to calculate the functions in Table 2 are compared in Table 7 to the corresponding values for the uranium dioxide system and the thorium dioxide system.

2. Hypostoichiometric Plutonium Dioxide

The free energy of formation of the hypostoichiometric condensed phase, $\Delta G_f^\circ(PuO_{2-x},c)$, can be calculated at any temperature from the free energy of formation of $PuO_2(c)$ and the oxygen potential using the following relationship:

$$\Delta G_f^\circ(PuO_{2-x},c) = \Delta G_f^\circ(PuO_2,c) - \frac{RT}{2} \int_0^x \ln p(O_2)\, dx' \tag{41}$$

This relationship, which is applicable provided that no phase boundaries are crossed at T between $x = 0$ and $x = x'$, arises from the Gibbs-Duhem equation and has been successfully used for the U/O system. [1] All calculated partial pressures depend upon the evaluation of Eq. (41) because of the interdependence of the various equilibria--Eqs. (7)-(10).

The evaluation of the integral in Eq. (41) differs from the corresponding integral for the U/O system because of the differences in the oxygen-potential models. In particular, the neglect of Pu^{6+}, but not U^{6+}, leads to the problem that $\ln p(O_2)$ for the Pu/O system becomes infinite as x goes to zero. However, the integral in Eq. (41) remains finite and has been evaluated in the following way.

We let I be the integral of $\ln p(O_2)$, which is defined in Eq. (19), between the lower and upper limits of integration a and b, respectively. We set $b = 0.005$, because Eq. (19) is well behaved for $x > 0.005$, and found the limit of I as $a \longrightarrow 0$. In this way, Eq. (41) may be evaluated by adding the integral between the limits 0.005 and x to the integral between the limits $x = 0$ and $x = 0.005$. Hence,

$$I = \int_a^b \ln p(O_2)\, dx$$

$$= 4 \int_a^b \ln (1 - 2x)\, dx - 4 \int_a^b \ln (2x)\, dx + 2 \int_a^b \ln (2 - x)\, dx + \int_a^b (A + B/T)\, dx$$

$$= 0.005(A + B/T) + 0.11892 \qquad (42)$$

where A may be either A_s or A_ℓ, depending on the region of the phase diagram (and similarly for B); b = 0.005; a = 0; and $\lim_{z \to 0} (z \cdot \ln z) = 0$.

By applying Eqs. (41) and (42), we have obtained $\Delta G_f^\circ (PuO_{2-x}, c)$ for each of the regions of the phase diagram that are defined in Fig. 4:

$$\Delta G_f^\circ(PuO_{2-x}, s) = \Delta G_f^\circ(PuO_2, s) - \Delta(0,x) \qquad (43)$$
for Regions I and II

$$\Delta G_f^\circ(PuO_{2-z}, s) = \Delta G_f^\circ(PuO_{2-y}, \ell) + \phi \qquad (44)$$

$$= \Delta G_f^\circ(PuO_2, s) - \Delta(0,z)$$
for Region III with $z < x < y$

$$\Delta G_f^\circ(PuO_{2-x}, \ell) = \Delta G_f^\circ(PuO_2, s) - \Delta(0,z) - \Delta(y,x) - \phi \qquad (45)$$
for Region IV with $z < y < x$

and

$$\Delta G_f^\circ(PuO_{2-x}, \ell) = \Delta G_f^\circ(UO_2, \ell) - \Delta(0,x) \qquad (46)$$
for Region V

where

$$\Delta(a,b) \equiv \frac{RT}{2} \int_a^b \ln p(O_2)\, dx \qquad (47)$$

and

$$\phi = \frac{y - z}{2} RT \ln p(O_2) \qquad (48)$$

and the overall composition of the system is O/Pu = 2 - x in all cases.

F. Ions

The extent to which ionization contributes to the vapor in equilibrium with a PuO_{2-x} condensed phase depends upon several factors, including the ionization potentials of the vapor species; the population of vibrational, rotational, and electronic states at the temperature of interest; and the partial pressure of each species in the vapor.

The ionization potential of each vapor species is given in Table 8. These data, a comparison with the U/O system, and the results obtained in the following sections of this report lead us to the conclusion that ionization can be neglected for the temperature and composition ranges of interest.

Table 8. Ionization Potentials (IP) of the Molecules and Atoms in Equilibrium with a Plutonium Dioxide Condensed Phase. ($1\ eV \cdot molecule^{-1} = 23.06\ kcal \cdot mol^{-1} = 96.48\ kJ \cdot mol^{-1}$)

Species	IP, eV	Reference
Pu	5.83	Report NSRDS-NBS 34 [46]
PuO	6.2 ± 0.5	Blackburn et al. [47]
PuO_2	9.4 ± 0.5	Blackburn et al. [47]
O	13.61	Moore [48]
O_2	12.07	Huber and Herzberg [49]

If additional data were obtained that required reexamination of this conclusion, then both Eqs. (1) and (2) would need to include additional terms. Because the partial pressures of the neutral species are unaffected by the presence or absence of ions, the total pressure, from Eq. (1), would increase if the partial pressure of any ionized species were important. The vapor composition would almost certainly become less oxygen-rich, i.e., R(gas) from Eq. (2) would decrease, because the lower ionization potentials in Table 8 are those of plutonium-containing species.

The ionization potentials in Table 8 are similar to their counterparts in the U/O system. [1] Ionization was shown to be of minor importance for the U/O system in the temperature and composition ranges of interest. For the Pu/O system, the composition range of interest is similar to that of the U/O system, and the upper temperature limit will be lower for the Pu/O system because of the limitations of the oxygen-potential model that were discussed in Section II.C.3. Thus, we may reasonably expect that ionization will be less important for the Pu/O system than for the U/O system.

Furthermore, the results obtained in Table 5 from the oxygen-potential model alone indicate that the vapor composition for the Pu/O system will be as oxygen-rich or more oxygen-rich than that for the U/O system. A very oxygen-rich equilibrium vapor gives less ionization because of the relatively high ionization potentials of O and O_2.

We shall not include ionization effects in our calculations.

III. RESULTS

The partial pressures of O, O_2, Pu, PuO, and PuO_2 were calculated as functions of T ($1500 \leq T \leq 4000$ K) and x ($0.005 < x < 0.30$), with particular emphasis on $0.005 < x < 0.10$. Preliminary calculations to 5000 K yielded unreasonably high oxygen pressures and vapor densities such that an upper temperature limit of 4000 K was selected. Tables presenting selected results are given in the Appendix. These calculated partial pressures and quantities derived from them were used to plot the figures discussed below.

The calculated composition of the vapor in equilibrium with a $PuO_{1.96}$ condensed phase, which is a typical composition for a reactor fuel, is shown in Fig. 5. Below 2652 K, which is the temperature at which $PuO_{1.96}$ begins to melt, the vapor is PuO_2 with varying amounts of PuO, O, and O_2. Above 2668 K,

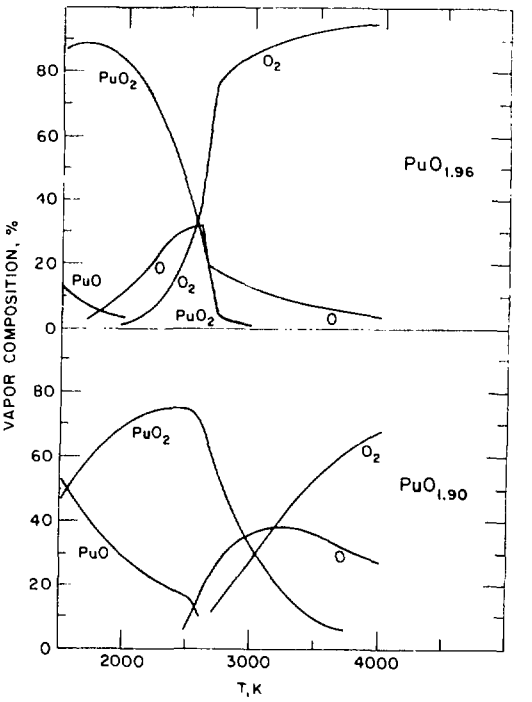

Fig. 5. Vapor Composition in Equilibrium with a $PuO_{1.96}$ Condensed Phase (top) and a $PuO_{1.90}$ Condensed Phase (bottom)

which is the liquidus temperature for $PuO_{1.96}$, the vapor is almost entirely O_2 with some O. None of the plutonium-containing species makes an appreciable contribution to the total pressure at high temperatures. The similarities and contrasts between the vapor composition in equilibrium with $PuO_{1.96}$ and that in equilibrium with $UO_{1.96}$ are discussed more fully in Section IV.A. Even the vapor in equilibrium with $PuO_{1.90}$, which is shown in the bottom part of Fig. 5, is largely O_2 and O at temperatures above 3000 K.

An alternative way to view the oxygen enrichment of the vapor relative to the condensed phase is to calculate the oxygen-to-plutonium ratio of the gas, R(gas), with Eq. (2). The O/Pu ratio of the gas phase exceeds that of the condensed phase with which it is in equilibrium by such a large amount that a plot of R(gas) vs. the condensed-phase O/Pu, comparable to Fig. 5 in ANL-CEN-RSD-81-1 [1] for the U/O system, is of little value. Like the U/O system, this oxygen enrichment of the vapor relative to the condensed phase is increasing with temperature. One implication of these results is that the condensed-phase and vapor-phase compositions will depend upon the extent of vaporization of a sample with overall composition given by O/Pu = 2 - x.

The temperature dependences of the total vapor pressures in equilibrium with the condensed-phase compositions $PuO_{1.90}$, $PuO_{1.96}$, and $PuO_{1.994}$ are compared in Fig. 6. The differences shown in Fig. 6 are due to the differences in oxygen pressures for the different compositions.

The uncertainties and the implications of these results are discussed more fully in the next section.

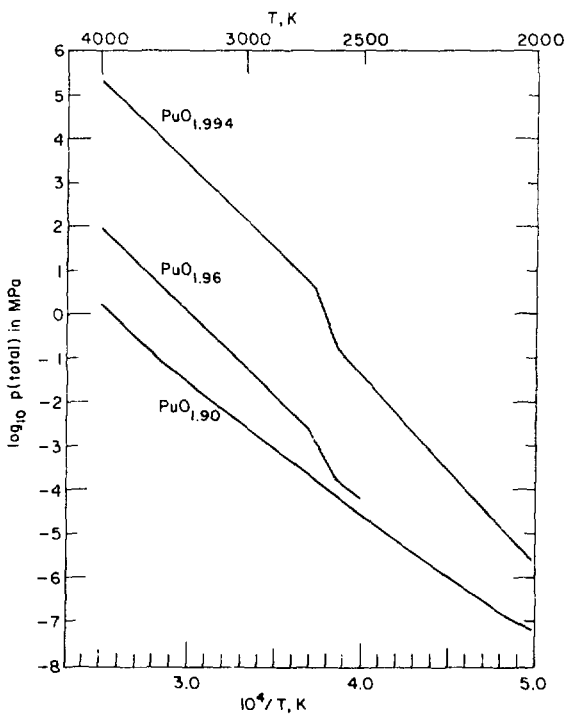

Fig. 6. Total Pressure in Equilibrium with $PuO_{1.994}$, $PuO_{1.96}$, and $PuO_{1.90}$

IV. DISCUSSION AND CONCLUSIONS

A. Comparison to the Uranium/Oxygen System

Comparison of the results of these calculations with those for the U/O system shows that the major difference is the very high oxygen pressures calculated for the plutonium oxides. Some of these data are compared in Table 9 for T = 2100 K and 4000 K. The oxygen pressures in equilibrium with PuO_{2-x} at 4000 K are higher than those in equilibrium with UO_{2-x} by factors ranging from about 10^6 to 10^3 for O/M ratios ranging from 1.98 to 1.90. At 2100 K, where experimental oxygen potentials are available, these same factors vary by 10^{10} to 10^8. Thus, the oxygen potentials for the two materials are actually getting closer as the temperature increases. When compared with available experimental data, the high oxygen pressures for equilibrium with PuO_{2-x} at 4000 K should not be at all surprising.

Table 9. Calculated Partial Pressures of O_2 at 2100 K and 4000 K for the U/O and Pu/O Systems

		Partial Pressure, MPa				
T,K	System	x = 0.02	x = 0.04	x = 0.06	x = 0.08	x = 0.10
2100	UO_{2-x}	3.4×10^{-18}	8.0×10^{-19}	3.3×10^{-19}	1.8×10^{-19}	1.3×10^{-19}
	PuO_{2-x}	1.2×10^{-8}	7.2×10^{-9}	1.2×10^{-9}	3.0×10^{-10}	9.8×10^{-11}
4000	UO_{2-x}	3.5×10^{-3}	1.9×10^{-3}	1.1×10^{-3}	7.1×10^{-4}	4.7×10^{-4}
	PuO_{2-x}	1.8×10^{3}	92	15	3.9	1.3

Another significant comparison between the two systems concerns the partial pressures of the metal dioxide molecules. These pressures are relatively insensitive to the condensed-phase composition and are quite similar in value for the plutonia and urania systems. Calculated metal dioxide vapor pressures for plutonia and urania are compared in Table 10 for O/M = 1.96. The sums of partial pressures of the metal-bearing species are also similar. This result would not have been easily predicted because each of the partial pressures is sensitive to $p(O_2)$, which is shown by the equilibria given in Eqs. (3)-(6). Some comparisons of these pressures are shown in Table 11, again for the O/M = 1.96 case. The conclusions based on the data in Tables 10 and 11 are reflections of the fact that the dioxide, in the range of temperatures and compositions being considered, is an important metal-bearing species.

As a consequence of the extreme sensitivity of oxygen pressure to stoichiometry for small values of x in PuO_{2-x}, the total pressure changes by a factor of about 10^3 in going from $PuO_{1.98}$ to $PuO_{1.90}$ at 4000 K. In contrast, the corresponding factor for the U/O system is approximately 2.

Table 10. Partial Pressures of the Dioxides in Equilibrium with the Hypostoichiometric Dioxides of Plutonium and Uranium

	Partial Pressure, MPa	
T,K	$PuO_{1.96}$	$UO_{1.96}$
2000	3.8×10^{-8}	1.2×10^{-8}
3000	1.0×10^{-3}	1.0×10^{-3}
4000	6.2×10^{-2}	7.8×10^{-2}

Table 11. Sums of Partial Pressures of Metal-bearing Species for the Pu/O and U/O Systems

	Partial Pressure, MPa	
T,K	$PuO_{1.96}$	$UO_{1.96}$
2000	3.9×10^{-8}	3.4×10^{-8}
3000	1.0×10^{-3}	1.1×10^{-3}
4000	6.2×10^{-2}	1.7×10^{-1}

The observation that the total pressure of the Pu/O system is much more sensitive to the condensed-phase composition than is that of the U/O system was pointed out in Section III.

It is important to consider the complex nature of the vapors in both oxide systems. Any analysis which considers only the dioxide partial pressures or approximates the total pressure as a dioxide pressure will be seriously in error.

B. Implications for Mixed Oxides

Because the oxygen potentials for the liquid plutonium oxide were so high, some preliminary calculations were performed for the mixed $(U,Pu)O_{2-x}$ system. Calculations were done by simultaneously solving the equations for the oxygen potentials for the Pu/O and U/O systems as described by Blackburn. [11] These results showed that, even though the plutonia system has an oxygen pressure larger than that for the comparable urania system (same composition and temperature) by a factor of 10^4 or 10^5, the mixed oxide containing 20% plutonia has an oxygen pressure only slightly greater than that for urania. Moreover, the pressure differences between the urania and mixed-oxide systems decreases as the temperature increases.

It appears that the presence of U^{6+}, for which there is no counterpart in the Pu/O system, is responsible for preventing the oxygen pressures from increasing as rapidly in the mixed system as in the plutonia system. Although considerable additional effort is needed to calculate reliable total pressures, our preliminary results indicate that the oxygen partial pressures in equilibrium with the mixed oxide will not differ drastically from those in equilibrium with urania.

C. Uncertainties and Limitations

The diagram of our calculational procedure given in Fig. 1 identifies the information that is essential for calculating vapor pressures and vapor compositions. There are uncertainties in the condensed-phase thermodynamic functions, in the oxygen-potential data and model, and in the gas-phase thermodynamic functions. However, the uncertainties in the oxygen-potential model far outweigh the uncertainties in the other two.

Of these three components of the calculation, the gas-phase thermodynamic functions have the smallest uncertainty. These uncertainties were discussed in detail in the report Calculation of the Thermodynamic Properties of Fuel-Vapor Species from Spectroscopic Data. [4] The effect of these uncertainties on the calculated vapor pressures at the upper temperature limit of 4000 K is expected to be less than a factor of two.

As discussed in Section II.E.1, the uncertainties in the condensed-phase thermodynamic functions arise from (1) the possible existence of a solid-solid phase transition in the temperature range 2160 to 2370 K and (2) the possible electronic contribution to the heat capacity of the liquid, which would give a heat capacity in the range of 122 to 132 $J \cdot mol^{-1} \cdot K^{-1}$ instead of the 96 $J \cdot mol^{-1} \cdot K^{-1}$ used in these calculations. While these uncertainties affect the partial pressures of plutonium oxides by a factor of 10 at 4000 K, they have no effect on the total pressure because, at that temperature, the total pressure is due essentially entirely to O_2 and O. If the oxygen-potential model were improved so that the contribution due to oxygen were limited, then this uncertainty in the condensed-phase thermodynamic functions would become a major uncertainty.

The large uncertainty in the results and the temperature limitations are due to the uncertainties in the oxygen-potential model that is used. Within this model several areas of uncertainty were identified and discussed. These are summarized below.

1. Neglect of Pu^{2+}. This uncertainty was discussed in Section II.C.1, where it is shown not to be a major contributor to the uncertainty. The effect of neglecting Pu^{2+} is illustrated in Table 3.

2. Neglect of Pu^{6+}. This uncertainty has been discussed in detail in Section II.C.1. Table 4 gives an estimate of its contribution as a function of temperature and stoichiometry. Table 4 shows that including Pu^{6+} changes the calculated pressures only by about 3% at 4000 K, but there are large uncertainties in the pressures that were calculated including a Pu^{6+} state. These uncertainties arise from the absence of experimental data on this state for the Pu/O system. The lack of any evidence of a hexavalent state in the Pu/O low-temperature data implies that the hexavalent state would have a steep

concentration gradient if it is important at 4000 K. Examination of the effect of a hexavalent state in the mixed-oxide system clearly shows its importance in limiting the oxygen partial pressures. Thus, the lack of experimental data on Pu^{6+} creates a major uncertainty in the oxygen-potential model.

3. Entropy estimates. The use of $\Delta S^\circ = 1.4$ nR instead of nR in the calculation of the liquid-phase parameters has been discussed in detail in Section II.C.2. Table 5 compares results for method B using both nR and 1.4 nR for ΔS°. At 3000 K, the difference for x = 0.1 is 8%. At 4000 K, the difference for x = 0.1 is 4%. This difference is small compared to the other uncertainties in the oxygen-potential model. The choice of 1.4 nR is the same as that made for the U/O system for similar reasons. [1]

4. Phase diagram. The phase diagram is used solely to determine the appropriate region for calculation of functions (e.g., integrations). Changes in the phase diagram would have small overall effects on the total pressures calculated. The phase diagram used is a result of choices of the parameters in the oxygen-potential model. Changes in these parameters would result in a modified phase diagram. Note that, although these parameters may give unreasonable results at high temperatures, the phase diagram that they give is not unreasonable. The existence of an independently determined phase diagram may be useful in the derivation of more reasonable oxygen-potential model parameters by the same methods that were used for the U/O system. [1] However, if there are still problems with the lack of information about the oxygen-potential model, such as the absence of reliable information on the hexavalent Pu state, a new phase diagram will not alleviate the problem.

5. Uncertainty in the method used to evaluate the model parameters for the oxygen potential of the liquid. This uncertainty is discussed in detail in Section II.C.2. Table 5 gives results for different methods. The method that was chosen has been compared with the method used for the U/O system. For the U/O system, the parameters calculated by the same method used for the Pu/O system differ by 8% from those calculated using the phase diagram of U/O. Above the melting point of UO_2, 3120 K, these parameters give total pressures for the U/O system that are a factor of 2 less than those calculated by the method used for the U/O system. [1] Thus, our choices of constants for the liquid system are expected to give low total pressures rather than unusually high ones. This error in underestimating the total pressure in the liquid region, which results from the method used to determine the liquid model parameters, is more than offset by deficiencies in the oxygen-potential model, including the exclusion of a higher oxidation state which creates unrealistically high pressures at high temperatures.

6. Neglect of ions. The contributions due to ions are discussed in Section II.F. As for the U/O system, the ion contribution for the Pu/O system is insignificant compared to the other uncertainties in the oxygen-potential model.

In summary, the limitation of our calculations to temperatures less than 4000 K is a consequence of excessive oxygen partial pressures, which are, in turn, the result of the oxygen-potential model or the model parameters that are used. Uncertainties in the gas-phase thermodynamic functions are not

important, and the uncertainties in the condensed-phase thermodynamic functions are not limiting. The unrealistically high oxygen pressures may be partially attributable to the lack of experimental data on a Pu^{6+} state (or other higher valence states). Furthermore, high-temperature experimental data are required to test the model employed here and, if necessary, modify it. If this problem with the oxygen-potential model is solved, then the limiting source of error would be the condensed-phase thermodynamic functions.

D. Possible Additional Work

At numerous points in this report we have pointed out that the limited experimental data for the Pu/O system prevent the calculation of results whose reliability is comparable to those for the U/O system. [1] It is not difficult to suggest areas where additional work would be useful.

Each of the major uncertainties discussed in Section IV.C could be reduced by additional experimental or theoretical work. The following list includes some of the specific areas where further work may be feasible and useful:

1. Measurement of the heat capacities of both solid and liquid condensed phase. The heat-capacity uncertainty is relatively unimportant to our calculations at high temperatures because of the much larger uncertainty in the oxygen potential; nevertheless, there is need for additional work. The uncertainty in the heat capacity affects the calculated partial pressures of the plutonium-containing species (Section IV.C). Thus, should some reasonable method be found to reduce the uncertainty in the oxygen potential, the uncertainty in the heat capacity could become limiting.

2. Measurement of the oxygen pressure or oxygen potential near stoichiometry at lower temperatures. Some data are available, but additional data would help establish their reliabilllity in the extremely important region near O/Pu = 2. There are well-known experimental problems associated with compositions near stoichiometry, but these data are extremely important to our understanding of the Pu/O vapor system because of the sensitivity of the oxygen potential to stoichiometry near O/Pu = 2. Thus, additional studies would be useful.

3. Measurement of the equilibrium oxygen pressure (as functions of both T and x) at higher temperatures than are currently available. Any additional reliable data would help reduce the large uncertainty that now exists (see Section IV.C). Oxygen potentials for the liquid phase would be particularly useful.

4. Measurement of the O/Pu ratio of the vapor in equilibrium with the plutonium dioxide liquid. This information, or any similar data, would help reduce the uncertainty in the oxygen potentials, which is the largest uncertainty.

5. Measurement of a more reliable phase diagram for the plutonium/oxygen system, particularly near the melting region. Although we have done the calculations in such a way that the phase diagram is a consequence of the oxygen-potential model, it is possible to do the reverse. If the phase diagram were more accurately known, the oxygen-potential model would have to be consistent with it. Thus, more reliable data on the phase diagram are of interest, primarily because they would help reduce the uncertainty in the oxygen potentials.

In summary, with the currently available information, the largest uncertainty is in the oxygen-potential model and the parameter values within the model. Additional work in other areas is of little value to the calculations at high temperature unless it contributes to reducing the uncertainty in the oxygen pressure at high temperatures.

ACKNOWLEDGMENTS

We gratefully acknowledge helpful discussions with Drs. P. E. Blackburn, M. Tetenbaum, and M.-L. Saboungi.

REFERENCES

1. D. W. Green and L. Leibowitz, Vapor Pressures and Vapor Compositions in Equilibrium with Hypostoichiometric Uranium Dioxide at High Temperatures, Argonne National Laboratory Report ANL-CEN-RSD-81-1 (1981); J. Nucl. Mater., 104, 196 (1982).

2. P. E. Potter and M. H. Rand, High Temp. Sci. 13, 315 (1980).

3. M. Rand, in Plutonium: Physico-Chemical Properties of its Compounds and Alloys, O. Kubaschewski, Ed., Atomic Energy Review, Vol. 4, Special Issue No. 1, International Atomic Energy Agency, Vienna, p. 7 (1966).

4. D. W. Green, Calculation of the Thermodynamic Properties of Fuel-Vapor Species from Spectroscopic Data, Argonne National Laboratory Report ANL-CEN-RSD-80-2 (1980).

5. JANAF Thermochemical Tables, 2nd Ed., Nat. Bur. of Std. Rept. NSRDS-NBS 37 (1971); 1974 Suppl., J. Phys. Chem. Ref. Data 3, 311 (1974); 1975 Suppl., J. Phys. Chem. Ref. Data 4, 1 (1975); 1978 Suppl., J. Phys. Chem. Ref. Data 7, 793 (1978).

6. F. L. Oetting, M. H. Rand, and R. J. Ackermann, The Chemical Thermodynamics of Actinide Elements and Their Compounds, International Atomic Energy Agency, Vienna (1976).

7. L. M. Atlas and G. J. Schlehman, in Thermodynamics of Nuclear Materials, International Atomic Energy Agency, Vienna, p. 407 (1966).

8. L. Manes and B. Manes-Pozzi, in Plutonium 1975 and Other Actinides, H. Blank and R. Linder, Ed., North Holland, Amsterdam, p. 145 (1976).

9. P. Browning, M. J. Gillan, and P. E. Potter, Rev. Int. Hautes Temp. Refract. 15, 333 (1978).

10. L. Manes, C. M. Mari, I. Ray, and O. T. Sorensen, in Thermodynamics of Nuclear Materials, International Atomic Energy Agency, Vienna, p. 405 (1979).

11. (a) P. E. Blackburn, in Chemical Engineering Division Fuels and Materials Chemistry Semiannual Report, July-December 1972, Argonne National Laboratory Report ANL-7977, p.12 (1972); (b) P. E. Blackburn, in Chemical Engineering Division Fuels and Materials Annual Report, July 1974-June 1975, ANL-75-48, p. 5 (1975); (c) P. E. Blackburn and C. E. Johnson, in Thermodynamics of Nuclear Materials, International Atomic Energy Agency, Vienna, p. 17 (1974).

12. (a) F. Schmitz, J. Nucl. Mater. 58, 357 (1975); (b) F. Schmitz and A. Marajofski, in Thermodynamics of Nuclear Materials, International Atomic Energy Agency, Vienna, p. 457 (1974).

13. W. Breitung, Kernforschungszentrum Karlsruhe Report KFK-2363 (1976).

14. M. de Franco and J. P. Gatsoupe, in Plutonium 1975 and Other Actinides, H. Blank and R. Linder, Ed., North Holland, Amsterdam, p. 133 (1976).

15. (a) C. R. A. Catlow, J. Nucl. Mater. 67, 236 (1977); (b) C. R. A. Catlow, J. Nucl. Mater. 74, 172 (1978).

16. L. Manes and Hj. Matzke, J. Nucl. Mater. 74, 167 (1978).

17. C. A. Alexander (Battelle Memorial Institute, Columbus Laboratories), data presented at the Libby-Cockcroft Exchange Meeting on Phase Diagrams and Thermodynamics of Fuel Materials, May 20-22, 1968.

18. T. L. Markin and E. J. McIver, in Plutontium 1965, A. E. Kay and M. B. Waldron, Ed., Chapman and Hall, London, p. 845 (1967).

19. R. E. Woodley, J. Amer. Ceram. Soc. 56, 116 (1973).

20. N. A. Javed, J. Nucl. Mater. 47, 336 (1973).

21. M. Tetenbaum, in Thermodynamics of Nuclear Materials, Vol. II, International Atomic Energy Agency, Vienna, p. 305 (1974); private communciation, 1973.

22. P. E. Blackburn, in Proc. Panel on Behavior and Chemical State of Irradiated Ceramic Fuels, International Atomic Energy Agency, Vienna, p. 393 (1974).

23. M. Tetenbaum, private communication (1981).

24. R. J. Ackermann and E. G. Rauh, J. Chem. Thermodyn. 3, 609 (1971).

25. International Atomic Energy Agency, The Plutonium-Oxygen and Uranium-Plutonium-Oxygen Systems: A Thermochemical Assessment, Tech. Report Ser. No. 79, International Atomic Energy Agency, Vienna (1967).

26. J. E. Battles and W. A. Shinn, in Chemical Engineering Division Research Highlights January-December 1969, Argonne National Laboratory Report ANL-7650, p. 23 (1970).

27. D. W. Green and G. T. Reedy, J. Chem. Phys. 69, 544 (1978).

28. D. W. Green and G. T. Reedy, unpublished results.

29. J. E. Battles, J. W. Reishus, and W. A. Shinn, in Chemical Engineering Division Annual Report, 1968, Argonne National Laboratory Report ANL-7575, p. 77 (1969).

30. D. T. Livey and P. Feschotte, in Plutonium: Physico-Chemical Properties of its Compounds and Alloys, O. Kubaschewski, Ed., Atomic Energy Review, Vol. 4, Special Issue No. 1, International Atomic Energy Agency, Vienna, p. 53 (1966).

31. E. A. Aitken and S. K. Evans, General Electric Reports GEAP-5672 (1968); a correction of 17 K to the melting point should be made, M. G. Adamson, private communication (1982).

32. J. K. Fink, "Enthalpy and Heat Capacity of Actinide Oxides," Int. J. Thermophysics 3, No. 2, 165 (1982).

33. M. H. Rand, in Thorium: Physico-Chemical Properties of its Compounds and Alloys, O. Kubaschewski, Ed., Atomic Energy Review, Special Issue No. 5, International Atomic Energy Agency, Vienna, p. 7 (1975).

34. M. H. Rand, R. J. Ackermann, F. Grønvold, F. L. Oetting, and A. Pattoret, Rev. Int. Hautes Temp. Réfract. 15, 355 (1978).

35. G. K. Johnson and W. V. Steele, J. Chem. Thermodyn. 13, 717 (1981).

36. H. E. Flotow, D. W. Osborne, S. A. Fried, and J. G. Malm, J. Chem. Phys. 65, 1124 (1976).

37. D. W. Osborne and E. F. Westrum, J. Chem. Phys. 21, 1884 (1953).

38. J. K. Fink, M. G. Chasanov, and L. Leibowitz, Thermodynamic Properties of Uranium Dioxide, Argonne National Laboratory Report ANL-CEN-RSD-80-3, (1981).

39. J. K. Fink, calculated with data in [32] and with data from Section II.E of this report.

40. D. F. Fischer, J. K. Fink, and L. Leibowitz, J. Nucl. Mater. 102, 220 (1981).

41. A. E. Ogard, in Plutonium 1970 and Other Actinides, W. N. Miner, Ed., Vol. 1, Metallurgical Soc., AIMNPE, New York, p. 78 (1970).

42. W. D. Drotning, in Proc. 8th Symposium on Thermophysical Properties, Am. Soc. Mech. Engr., to be published.

43. J. K. Fink, M. G. Chasanov, and L. Leibowitz, The Enthalpy and Heat Capacity of Solid UO_2, Argonne National Laboratory Report ANL-CEN-RSD-81-2 (1981).

44. R. A. Young, J. Nucl. Mater. 87, 283 (1979).

45. e.g., J. C. Slater, Introduction to Chemical Physics, McGraw-Hill, New York, p. 220 (1939).

46. C. E. Moore, National Bureau of Standards (U.S.) Report NSRDS-NBS 34 (1970).

47. P. E. Blackburn, J. E. Battles, J. W. Reushus, and W. A. Shinn, in Chemical Engineering Division Annual Report, 1968 Argonne National Laboratory Report ANL-7575, p. 79 (1969).

48. C. E. Moore, Atomic Energy Levels, National Bureau of Standards, Circular 467, Washington, D.C. (1949).

49. K. P. Huber and G. Herzberg, Molecular Spectra and Molecular Structure IV. Constants of Diatomic Molecules, Van Nostrand Reinhold, New York (1979).

APPENDIX

CALCULATED PARTIAL PRESSURES IN EQUILIBRIUM WITH A PuO_{2-x} CONDENSED PHASE

Each of the following tables contains the calculated partial pressures and total pressure (in MPa) in equilibrium with PuO_{2-x} as a function of temperature for $1500 < T < 4000$ K for one value of x between $x = 0.10$ and $x = 0.006$. The applicable regions of the phase diagram, as defined in Fig. 4, are given in the tables. These pressures were calculated with a program called TOTPU, which is based on the methods and data described in this report. Program TOTPU for the Pu/O system is similar to program TOTPR for the U/O system. Numerical integrations to obtain $\Delta G_f^\circ(PuO_{2-x},c)$ were done with subroutine SQUANK (J. N. Lyness and K. E. Hillstrom, Argonne National Laboratory, Applied Mathematics Division, July 1970).

Table A-1. Partial Pressures and Total Pressure (in MPa) in Equilibrium with a $PuO_{1.994}$ Condensed Phase

T,K	REG[a]	$p(O_2)$	p(O)	$p(PuO_2)$	p(PuO)	p(Pu)	p(total)
1500	I	0.7664D-13	0.3547D-12	0.5981D-12	0.1589D-14	0.4881D-22	0.1031D-11
1600	I	0.5284D-11	0.1053D-10	0.9889D-11	0.2035D-13	0.6875D-21	0.2573D-10
1700	I	0.2214D-09	0.2101D-09	0.1162D-09	0.1905D-12	0.7040D-20	0.5478D-09
1800	I	0.6126D-08	0.3008D-08	0.1026D-08	0.1373D-11	0.5530D-19	0.1016D-07
1900	I	0.1195D-06	0.3258D-07	0.7132D-08	0.7945D-11	0.3476D-18	0.1592D-06
2000	I	0.1732D-05	0.2782D-06	0.4042D-07	0.3813D-10	0.1808D-17	0.2051D-05
2100	I	0.1946D-04	0.1938D-05	0.1924D-06	0.1559D-09	0.7999D-17	0.2159D-04
2200	I	0.1755D-03	0.1132D-04	0.7873D-06	0.5549D-09	0.3077D-16	0.1876D-03
2300	I	0.1307D-02	0.5675D-04	0.2826D-05	0.1751D-08	0.1048D-15	0.1366D-02
2400	I	0.8233D-02	0.2488D-03	0.9041D-05	0.4974D-08	0.3212D-15	0.8491D-02
2500	II	0.4477D-01	0.9692D-03	0.2615D-04	0.1288D-07	0.8964D-15	0.4573D-01
2600	II	0.2137D+00	0.3402D-02	0.6915D-04	0.3072D-07	0.2304D-14	0.2172D+00
2700	IV	0.5525D+01	0.2684D-01	0.1689D-03	0.2763D-07	0.9047D-15	0.5552D+01
2800	V	0.1797D+02	0.7278D-01	0.3359D-03	0.5449D-07	0.2085D-14	0.1804D+02
2900	V	0.5388D+02	0.1843D+00	0.6245D-03	0.1004D-06	0.4464D-14	0.5407D+02
3000	V	0.1502D+03	0.4387D+00	0.1112D-02	0.1771D-06	0.9101D-14	0.1506D+03
3100	V	0.3917D+03	0.9874D+00	0.1904D-02	0.3004D-06	0.1775D-13	0.3927D+03
3200	V	0.9623D+03	0.2113D+01	0.3147D-02	0.4917D-06	0.3328D-13	0.9644D+03
3300	V	0.2239D+04	0.4319D+01	0.5036D-02	0.7792D-06	0.6014D-13	0.2243D+04
3400	V	0.4956D+04	0.8463D+01	0.7828D-02	0.1199D-05	0.1052D-12	0.4965D+04
3500	V	0.1049D+05	0.1596D+02	0.1184D-01	0.1795D-05	0.1784D-12	0.1050D+05
3600	V	0.2128D+05	0.2906D+02	0.1749D-01	0.2622D-05	0.2943D-12	0.2131D+05
3700	V	0.4156D+05	0.5124D+02	0.2511D-01	0.3772D-05	0.4665D-12	0.4161D+05
3800	V	0.7835D+05	0.8767D+02	0.3537D-01	0.5251D-05	0.7276D-12	0.7844D+05
3900	V	0.1430D+06	0.1460D+03	0.4886D-01	0.7176D-05	0.1110D-11	0.1432D+06
4000	V	0.2533D+06	0.2369D+03	0.6629D-01	0.9639D-05	0.1659D-11	0.2535D+06

[a]Region defined in Fig. 4.

Table A-2. Partial Pressures and Total Pressure (in MPa) in Equilibrium with a $PuO_{1.98}$ Condensed Phase

T,K	REG[a]	$p(O_2)$	$p(O)$	$p(PuO_2)$	$p(PuO)$	$p(Pu)$	p(total)
1500	I	0.5456D-15	0.2993D-13	0.5811D-12	0.1830D-13	0.6662D-20	0.6299D-12
1600	I	0.3762D-13	0.8886D-12	0.9608D-11	0.2344D-12	0.9383D-19	0.1077D-10
1700	I	0.1576D-11	0.1773D-10	0.1129D-09	0.2194D-11	0.9608D-18	0.1344D-09
1800	I	0.4361D-10	0.2538D-09	0.9970D-09	0.1581D-10	0.7547D-17	0.1310D-08
1900	I	0.8507D-09	0.2749D-08	0.6929D-08	0.9149D-10	0.4744D-16	0.1062D-07
2000	I	0.1233D-07	0.2347D-07	0.3928D-07	0.4390D-09	0.2468D-15	0.7552D-07
2100	I	0.1385D-06	0.1635D-06	0.1869D-06	0.1795D-08	0.1092D-14	0.4908D-06
2200	I	0.1249D-05	0.9552D-06	0.7649D-06	0.6389D-08	0.4199D-14	0.2976D-05
2300	I	0.9303D-05	0.4788D-05	0.2745D-05	0.2016D-07	0.1431D-13	0.1686D-04
2400	I	0.5861D-04	0.2099D-04	0.8784D-05	0.5728D-07	0.4384D-13	0.8844D-04
2500	II	0.3187D-03	0.8178D-04	0.2540D-04	0.1483D-06	0.1223D-12	0.4260D-03
2600	II	0.1521D-02	0.2870D-03	0.6718D-04	0.3538D-06	0.3144D-12	0.1876D-02
2700	IV	0.3933D-01	0.2264D-02	0.1641D-03	0.3182D-06	0.1235D-12	0.4176D-01
2800	V	0.1279D+00	0.6141D-02	0.3263D-03	0.6274D-06	0.2846D-12	0.1344D+00
2900	V	0.3836D+00	0.1555D-01	0.6067D-03	0.1156D-05	0.6092D-12	0.3998D+00
3000	V	0.1069D+01	0.3701D-01	0.1080D-02	0.2040D-05	0.1242D-11	0.1107D+01
3100	V	0.2789D+01	0.8331D-01	0.1850D-02	0.3460D-05	0.2423D-11	0.2874D+01
3200	V	0.6851D+01	0.1783D+00	0.3057D-02	0.5662D-05	0.4541D-11	0.7032D+01
3300	V	0.1594D+02	0.3644D+00	0.4893D-02	0.8972D-05	0.8208D-11	0.1631D+02
3400	V	0.3528D+02	0.7141D+00	0.7605D-02	0.1380D-04	0.1435D-10	0.3601D+02
3500	V	0.7464D+02	0.1347D+01	0.1151D-01	0.2067D-04	0.2434D-10	0.7600D+02
3600	V	0.1515D+03	0.2452D+01	0.1699D-01	0.3019D-04	0.4017D-10	0.1539D+03
3700	V	0.2958D+03	0.4323D+01	0.2439D-01	0.4344D-04	0.6367D-10	0.3002D+03
3800	V	0.5578D+03	0.7397D+01	0.3436D-01	0.6047D-04	0.9931D-10	0.5652D+03
3900	V	0.1018D+04	0.1231D+02	0.4747D-01	0.8263D-04	0.1515D-09	0.1030D+04
4000	V	0.1803D+04	0.1999D+02	0.6440D-01	0.1110D-03	0.2264D-09	0.1823D+04

[a]Region defined in Fig. 4.

Table A-3. Partial Pressures and Total Pressure (in MPa) in Equilibrium with a $PuO_{1.96}$ Condensed Phase

T,K	REG[a]	$p(O_2)$	$p(O)$	$p(PuO_2)$	$p(PuO)$	$p(Pu)$	p(total)
1500	I	0.2819D-16	0.6803D-14	0.5568D-12	0.7714D-13	0.1235D-18	0.6407D-12
1600	I	0.1943D-14	0.2020D-12	0.9205D-11	0.9879D-12	0.1740D-17	0.1040D-10
1700	I	0.8142D-13	0.4029D-11	0.1081D-09	0.9247D-11	0.1782D-16	0.1215D-09
1800	I	0.2253D-11	0.5769D-10	0.9552D-09	0.6666D-10	0.1400D-15	0.1082D-08
1900	I	0.4395D-10	0.6247D-09	0.6638D-08	0.3856D-09	0.8798D-15	0.7693D-08
2000	I	0.6369D-09	0.5335D-08	0.3763D-07	0.1851D-08	0.4576D-14	0.4545D-07
2100	I	0.7156D-08	0.3716D-07	0.1791D-06	0.7566D-08	0.2025D-13	0.2310D-06
2200	I	0.6453D-07	0.2171D-06	0.7328D-06	0.2693D-07	0.7788D-13	0.1041D-05
2300	I	0.4806D-06	0.1088D-05	0.2630D-05	0.8500D-07	0.2653D-12	0.4284D-05
2400	I	0.3028D-05	0.4771D-05	0.8415D-05	0.2415D-06	0.8130D-12	0.1646D-04
2500	II	0.1646D-04	0.1859D-04	0.2434D-04	0.6252D-06	0.2269D-11	0.6001D-04
2600	II	0.7859D-04	0.6524D-04	0.6436D-04	0.1491D-05	0.5831D-11	0.2097D-03
2700	IV	0.2032D-02	0.5146D-03	0.1572D-03	0.1341D-05	0.2290D-11	0.2705D-02
2800	V	0.6609D-02	0.1396D-02	0.3127D-03	0.2645D-05	0.5278D-11	0.8320D-02
2900	V	0.1982D-01	0.3534D-02	0.5812D-03	0.4874D-05	0.1130D-10	0.2394D-01
3000	V	0.5522D-01	0.8412D-02	0.1035D-02	0.8598D-05	0.2304D-10	0.6468D-01
3100	V	0.1440D+00	0.1894D-01	0.1772D-02	0.1458D-04	0.4494D-10	0.1648D+00
3200	V	0.3539D+00	0.4052D-01	0.2929D-02	0.2387D-04	0.8422D-10	0.3974D+00
3300	V	0.8233D+00	0.8282D-01	0.4688D-02	0.3782D-04	0.1522D-09	0.9109D+00
3400	V	0.1823D+01	0.1623D+00	0.7286D-02	0.5818D-04	0.2662D-09	0.1992D+01
3500	V	0.3856D+01	0.3061D+00	0.1103D-01	0.8712D-04	0.4515D-09	0.4173D+01
3600	V	0.7825D+01	0.5573D+00	0.1628D-01	0.1273D-03	0.7449D-09	0.8398D+01
3700	V	0.1528D+02	0.9825D+00	0.2337D-01	0.1831D-03	0.1181D-08	0.1629D+02
3800	V	0.2881D+02	0.1681D+01	0.3292D-01	0.2549D-03	0.1842D-08	0.3053D+02
3900	V	0.5259D+02	0.2799D+01	0.4548D-01	0.3483D-03	0.2810D-08	0.5543D+02
4000	V	0.9314D+02	0.4542D+01	0.6170D-01	0.4678D-03	0.4199D-08	0.9774D+02

[a]Region defined in Fig. 4.

Table A-4. Partial Pressures and Total Pressure (in MPa) in Equilibrium with a $PuO_{1.94}$ Condensed Phase

T,K	REG[a]	$p(O_2)$	$p(O)$	$p(PuO_2)$	$p(PuO)$	$p(Pu)$	p(total)
1500	I	0.4566D-17	0.2738D-14	0.5323D-12	0.1832D-12	0.7291D-18	0.7182D-12
1600	I	0.3148D-15	0.8129D-13	0.8800D-11	0.2346D-11	0.1027D-16	0.1123D-10
1700	I	0.1319D-13	0.1622D-11	0.1034D-09	0.2196D-10	0.1052D-15	0.1270D-09
1800	I	0.3649D-12	0.2322D-10	0.9132D-09	0.1583D-09	0.8260D-15	0.1095D-08
1900	I	0.7119D-11	0.2515D-09	0.6347D-08	0.9160D-09	0.5192D-14	0.7521D-08
2000	I	0.1032D-09	0.2147D-08	0.3597D-07	0.4396D-08	0.2701D-13	0.4262D-07
2100	I	0.1159D-08	0.1496D-07	0.1712D-06	0.1797D-07	0.1195D-12	0.2053D-06
2200	I	0.1045D-07	0.8738D-07	0.7006D-06	0.6397D-07	0.4596D-12	0.8624D-06
2300	I	0.7785D-07	0.4380D-06	0.2514D-05	0.2019D-06	0.1566D-11	0.3232D-05
2400	I	0.4905D-06	0.1920D-05	0.8045D-05	0.5735D-06	0.4798D-11	0.1103D-04
2500	II	0.2667D-05	0.7481D-05	0.2327D-04	0.1485D-05	0.1339D-10	0.3490D-04
2600	II	0.1273D-04	0.2626D-04	0.6153D-04	0.3542D-05	0.3441D-10	0.1041D-03
2700	IV	0.3291D-03	0.2071D-03	0.1503D-03	0.3186D-05	0.1351D-10	0.6898D-03
2800	V	0.1071D-02	0.5617D-03	0.2989D-03	0.6282D-05	0.3115D-10	0.1937D-02
2900	V	0.3210D-02	0.1422D-02	0.5557D-03	0.1158D-04	0.6668D-10	0.5200D-02
3000	V	0.8946D-02	0.3386D-02	0.9894D-03	0.2042D-04	0.1359D-09	0.1334D-01
3100	V	0.2334D-01	0.7621D-02	0.1694D-02	0.3464D-04	0.2652D-09	0.3269D-01
3200	V	0.5733D-01	0.1631D-01	0.2800D-02	0.5669D-04	0.4970D-09	0.7650D-01
3300	V	0.1334D+00	0.3333D-01	0.4482D-02	0.8983D-04	0.8983D-09	0.1713D+00
3400	V	0.2953D+00	0.6532D-01	0.6966D-02	0.1382D-03	0.1571D-08	0.3677D+00
3500	V	0.6246D+00	0.1232D+00	0.1054D-01	0.2069D-03	0.2665D-08	0.7586D+00
3600	V	0.1268D+01	0.2243D+00	0.1556D-01	0.3023D-03	0.4396D-08	0.1508D+01
3700	V	0.2476D+01	0.3955D+00	0.2234D-01	0.4349D-03	0.6969D-08	0.2894D+01
3800	V	0.4668D+01	0.6767D+00	0.3148D-01	0.6054D-03	0.1087D-07	0.5377D+01
3900	V	0.8519D+01	0.1127D+01	0.4348D-01	0.8273D-03	0.1658D-07	0.9690D+01
4000	V	0.1509D+02	0.1826D+01	0.5899D-01	0.1111D-02	0.2478D-07	0.1698D+02

[a]Region defined in Fig. 4.

Table A-5. Partial Pressures and Total Pressure (in MPa) in Equilibrium with a $PuO_{1.92}$ Condensed Phase

T,K	REG[a]	$p(O_2)$	$p(O)$	$p(PuO_2)$	$p(PuO)$	$p(Pu)$	p(total)
1500	I	0.1175D-17	0.1389D-14	0.5077D-12	0.3445D-12	0.2703D-17	0.8536D-12
1600	I	0.8100D-16	0.4123D-13	0.8394D-11	0.4412D-11	0.3807D-16	0.1285D-10
1700	I	0.3394D-14	0.8225D-12	0.9860D-10	0.4130D-10	0.3899D-15	0.1407D-09
1800	I	0.9390D-13	0.1178D-10	0.8710D-09	0.2977D-09	0.3062D-14	0.1181D-08
1900	I	0.1832D-11	0.1275D-09	0.6054D-08	0.1723D-08	0.1925D-13	0.7906D-08
2000	I	0.2655D-10	0.1089D-08	0.3431D-07	0.8266D-08	0.1001D-12	0.4369D-07
2100	I	0.2983D-09	0.7587D-08	0.1633D-06	0.3379D-07	0.4429D-12	0.2050D-06
2200	I	0.2689D-08	0.4432D-07	0.6683D-06	0.1203D-06	0.1704D-11	0.8356D-06
2300	I	0.2003D-07	0.2222D-06	0.2398D-05	0.3797D-06	0.5805D-11	0.3020D-05
2400	I	0.1262D-06	0.9740D-06	0.7674D-05	0.1078D-05	0.1779D-10	0.9853D-05
2500	II	0.6862D-06	0.3795D-05	0.2219D-04	0.2792D-05	0.4964D-10	0.2947D-04
2600	II	0.3276D-05	0.1332D-04	0.5869D-04	0.6661D-05	0.1276D-09	0.8195D-04
2700	IV	0.8469D-04	0.1051D-03	0.1434D-03	0.5991D-05	0.5010D-10	0.3391D-03
2800	V	0.2754D-03	0.2849D-03	0.2851D-03	0.1181D-04	0.1155D-09	0.8573D-03
2900	V	0.8259D-03	0.7215D-03	0.5300D-03	0.2177D-04	0.2472D-09	0.2099D-02
3000	V	0.2302D-02	0.1717D-02	0.9437D-03	0.3840D-04	0.5040D-09	0.5001D-02
3100	V	0.6004D-02	0.3866D-02	0.1616D-02	0.6514D-04	0.9832D-09	0.1155D-01
3200	V	0.1475D-01	0.8273D-02	0.2671D-02	0.1066D-03	0.1843D-08	0.2580D-01
3300	V	0.3432D-01	0.1691D-01	0.4275D-02	0.1689D-03	0.3330D-08	0.5567D-01
3400	V	0.7597D-01	0.3314D-01	0.6644D-02	0.2599D-03	0.5823D-08	0.1160D+00
3500	V	0.1607D+00	0.6249D-01	0.1005D-01	0.3891D-03	0.9878D-08	0.2337D+00
3600	V	0.3261D+00	0.1138D+00	0.1484D-01	0.5684D-03	0.1630D-07	0.4553D+00
3700	V	0.6370D+00	0.2006D+00	0.2131D-01	0.8178D-03	0.2584D-07	0.8597D+00
3800	V	0.1201D+01	0.3432D+00	0.3002D-01	0.1138D-02	0.4029D-07	0.1575D+01
3900	V	0.2192D+01	0.5714D+00	0.4147D-01	0.1556D-02	0.6147D-07	0.2806D+01
4000	V	0.3882D+01	0.9274D+00	0.5627D-01	0.2090D-02	0.9187D-07	0.4868D+01

[a]Region defined in Fig. 4.

Table A-6. Partial Pressures and Total Pressure (in MPa) in Equilibrium with a $PuO_{1.90}$ Condensed Phase

T,K	REG[a]	$p(O_2)$	p(O)	$p(PuO_2)$	p(PuO)	p(Pu)	p(total)
1500	I	0.3877D-18	0.7978D-15	0.4831D-12	0.5707D-12	0.7794D-17	0.1055D-11
1600	I	0.2673D-16	0.2369D-13	0.7987D-11	0.7309D-11	0.1098D-15	0.1532D-10
1700	I	0.1120D-14	0.4725D-12	0.9381D-10	0.6841D-10	0.1124D-14	0.1627D-09
1800	I	0.3099D-13	0.6766D-11	0.8288D-09	0.4932D-09	0.8830D-14	0.1329D-08
1900	I	0.6044D-12	0.7327D-10	0.5760D-08	0.2853D-08	0.5550D-13	0.8687D-08
2000	I	0.8760D-11	0.6257D-09	0.3265D-07	0.1369D-07	0.2887D-12	0.4697D-07
2100	I	0.9842D-10	0.4359D-08	0.1554D-06	0.5597D-07	0.1277D-11	0.2158D-06
2200	I	0.8875D-09	0.2546D-07	0.6359D-06	0.1993D-06	0.4913D-11	0.8615D-06
2300	I	0.6610D-08	0.1276D-06	0.2282D-05	0.6289D-06	0.1674D-10	0.3045D-05
2400	I	0.4164D-07	0.5595D-06	0.7302D-05	0.1786D-05	0.5128D-10	0.9689D-05
2500	II	0.2264D-06	0.2180D-05	0.2112D-04	0.4625D-05	0.1431D-09	0.2815D-04
2600	III	0.2111D-05	0.1069D-04	0.5388D-04	0.7617D-05	0.1817D-09	0.7429D-04
2700	IV	0.2795D-04	0.6036D-04	0.1364D-03	0.9922D-05	0.1445D-09	0.2346D-03
2800	V	0.9090D-04	0.1637D-03	0.2713D-03	0.1957D-04	0.3329D-09	0.5454D-03
2900	V	0.2726D-03	0.4145D-03	0.5043D-03	0.3606D-04	0.7128D-09	0.1227D-02
3000	V	0.7596D-03	0.9865D-03	0.8979D-03	0.6361D-04	0.1453D-08	0.2708D-02
3100	V	0.1981D-02	0.2221D-02	0.1538D-02	0.1079D-03	0.2835D-08	0.5848D-02
3200	V	0.4868D-02	0.4752D-02	0.2541D-02	0.1766D-03	0.5313D-08	0.1234D-01
3300	V	0.1132D-01	0.9713D-02	0.4067D-02	0.2798D-03	0.9603D-08	0.2538D-01
3400	V	0.2507D-01	0.1903D-01	0.6322D-02	0.4304D-03	0.1679D-07	0.5086D-01
3500	V	0.5304D-01	0.3590D-01	0.9566D-02	0.6445D-03	0.2848D-07	0.9915D-01
3600	V	0.1076D+00	0.6537D-01	0.1412D-01	0.9415D-03	0.4699D-07	0.1881D+00
3700	V	0.2102D+00	0.1152D+00	0.2028D-01	0.1355D-02	0.7449D-07	0.3471D+00
3800	V	0.3963D+00	0.1972D+00	0.2857D-01	0.1886D-02	0.1162D-06	0.6240D+00
3900	V	0.7234D+00	0.3283D+00	0.3946D-01	0.2577D-02	0.1772D-06	0.1094D+01
4000	V	0.1281D+01	0.5327D+00	0.5354D-01	0.3461D-02	0.2649D-06	0.1871D+01

[a]Region defined in Fig. 4.